Key role of the scavenger receptor MARCO in mediating adenovirus infection and subsequent innate responses of macrophages

Maler, Mareike D ; Nielsen, Peter J ; Stichling, Nicole ; Cohen, Idan ; Ruzsics, Zsolt ; Wood, Connor ; Engelhard, Peggy ; Suomalainen, Maarit ; Gyory, Ildiko ; Huber, Michael ; Müller-Quernheim, Joachim ; Schamel, Wolfgang W A ; Gordon, Siamon ; Jakob, Thilo ; Martin, Stefan F ; Jahnen-Dechent, Willi ; Greber, Urs F ; Freudenberg, Marina A ; Fejer, György

Abstract: The scavenger receptor MARCO is expressed in several subsets of naive tissue-resident macrophages and has been shown to participate in the recognition of various bacterial pathogens. However, the role of MARCO in antiviral defense is largely unexplored. Here, we investigated whether MARCO might be involved in the innate sensing of infection with adenovirus and recombinant adenoviral vectors by macrophages, which elicit vigorous immune responses in vivo Using cells derived from mice, we show that adenovirus infection is significantly more efficient in MARCO-positive alveolar macrophages (AMs) and in AM-like primary macrophage lines (Max Planck Institute cells) than in MARCO-negative bone marrow-derived macrophages. Using antibodies blocking ligand binding to MARCO, as well as gene-deficient and MARCO-transfected cells, we show that MARCO mediates the rapid adenovirus transduction of macrophages. By enhancing adenovirus infection, MARCO contributes to efficient innate virus recognition through the cytoplasmic DNA sensor cGAS. This leads to strong proinflammatory responses, including the production of interleukin-6 (IL-6), alpha/beta interferon, and mature IL-1 . These findings contribute to the understanding of viral pathogenesis in macrophages and may open new possibilities for the development of tools to influence the outcome of infection with adenovirus or adenovirus vectors.IMPORTANCE Macrophages play crucial roles in inflammation and defense against infection. Several macrophage subtypes have been identified with differing abilities to respond to infection with both natural adenoviruses and recombinant adenoviral vectors. Adenoviruses are important respiratory pathogens that elicit vigorous innate responses in vitro and in vivo The cell surface receptors mediating macrophage type-specific adenovirus sensing are largely unknown. The scavenger receptor MARCO is expressed on some subsets of naive tissue-resident macrophages, including lung alveolar macrophages. Its role in antiviral macrophage responses is largely unexplored. Here, we studied whether the differential expression of MARCO might contribute to the various susceptibilities of macrophage subtypes to adenovirus. We demonstrate that MARCO significantly enhances adenovirus infection and innate responses in macrophages. These results help to understand adenoviral pathogenesis and may open new possibilities to influence the outcome of infection with adenoviruses or adenovirus vectors.

DOI: https://doi.org/10.1128/mBio.00670-17

Originally published at:
Maler, Mareike D; Nielsen, Peter J; Stichling, Nicole; Cohen, Idan; Ruzsics, Zsolt; Wood, Connor; Engelhard, Peggy; Suomalainen, Maarit; Gyory, Ildiko; Huber, Michael; Müller-Quernheim, Joachim; Schamel, Wolfgang W A; Gordon, Siamon; Jakob, Thilo; Martin, Stefan F; Jahnen-Dechent, Willi; Greber, Urs F; Freudenberg, Marina A; Fejer, György (2017). Key role of the scavenger receptor MARCO in mediating adenovirus infection and subsequent innate responses of macrophages. mBio, 8(4):e00670-17.
DOI: https://doi.org/10.1128/mBio.00670-17

Key role of the scavenger receptor MARCO in mediating adenovirus infection and subsequent innate responses of macrophages

Mareike D. Maler,[a,b,c] Peter J. Nielsen,[a] Nicole Stichling,[d] Idan Cohen,[a] Zsolt Ruzsics,[e] Connor Wood,[f] Peggy Engelhard,[g] Maarit Suomalainen,[d] Ildiko Gyory,[h] Michael Huber,[i] Joachim Müller-Quernheim,[g] Wolfgang W. A. Schamel,[j] Siamon Gordon,[k] Thilo Jakob,[b,l] Stefan F. Martin,[b] Willi Jahnen-Dechent,[m] Urs F. Greber,[d] Marina A. Freudenberg[a,g,j]# and György Fejer[a,f]#

Max-Planck-Institute of Immunobiology and Epigenetics, Freiburg, Germany[a]; Allergy Research Group, Department of Dermatology, Medical Center - University of Freiburg, Faculty of Medicine, University of Freiburg, Germany[b]; Faculty of Biology, University of Freiburg[c]; Institute of Molecular Life Sciences, University of Zurich, Zurich, Switzerland[d]; Institute for Virology, Medical Center - University of Freiburg, Faculty of Medicine, University of Freiburg, Freiburg Germany[e]; School of Biomedical and Healthcare Sciences, Peninsula Schools of Medicine and Dentistry, University of Plymouth, Plymouth, UK[f]; Department of Pneumology, Medical Center – University of Freiburg, Faculty of Medicine, University of Freiburg, Freiburg, Germany[g]; Department of Molecular and Cell Biology, University of Leicester, Leicester, UK[h]; Institute of Biochemistry and Molecular Immunology, University Clinic, RWTH Aachen University, Aachen, Germany[i]; BIOSS Centre for Biological Signalling Studies, Faculty of Biology, and Center for Chronic Immunodeficiency CCI, Medical Center– University of Freiburg, Faculty of Medicine, University of Freiburg, Freiburg, Germany[j]; Sir William Dunn School of Pathology, University of Oxford, Oxford, UK[k]; Department of Dermatology and

Allergology, University Medical Center Giessen and Marburg, Justus Liebig University Giessen[l];
Helmholtz Institute for Biomedical Engineering, Biointerface Laboratory, Aachen, Germany[m]

Running title: MARCO-mediated adenovirus infection & innate response

Address correspondence to Marina A. Freudenberg, marina.freudenberg@uniklinik-freiburg.de, BIOSS Centre for Biological Signalling Studies, Schänzlestr. 18, 79104 Freiburg, Germany and to György Fejer, gyorgy.fejer@plymouth.ac.uk, School of Biomedical and Healthcare Sciences, University of Plymouth, Drake Circus, PL4 8AA, Plymouth, UK

Abstract: 190 words

Text: 5768 words

Abstract

The scavenger receptor MARCO is expressed in several subsets of naïve tissue resident macrophages and has been shown to participate in the recognition of various bacterial pathogens. However, the role of MARCO in antiviral defence is largely unexplored. Here, we investigated whether MARCO might be involved in the innate sensing of infection with adenovirus and recombinant adenoviral vectors by macrophages, which elicit vigorous immune responses *in vivo*. Using cells derived from mice we show that adenovirus infection is significantly more efficient in MARCO-positive alveolar macrophages (AMs) and in AM-like primary macrophage lines (MPI cells) than in MARCO-negative bone marrow-derived macrophages. Using antibodies blocking ligand binding to MARCO, as well as gene-deficient and MARCO-transfected cells, we show that MARCO mediates the rapid adenovirus transduction of macrophages. By enhancing adenovirus infection, MARCO contributes to the efficient innate virus recognition through the cytoplasmic DNA sensor cGAS. This leads to strong pro-inflammatory responses including the production of IL-6, IFN-α/β and mature IL-1α. These findings contribute to the understanding of viral pathogenesis in macrophages and may open new possibilities for the development of tools to influence the outcome of infection with adenovirus or adenovirus vectors.

Importance

Macrophages play crucial roles in inflammation and defense against infection. Several macrophage subtypes have been identified with differing abilities to respond to infection with both natural adenoviruses as well as recombinant adenoviral vectors. Adenoviruses are important

71 respiratory pathogens, which elicit vigorous innate responses *in vitro* and *in vivo*. The cell surface
72 receptors mediating macrophage type specific adenovirus sensing are largely unknown.
73 The scavenger receptor MARCO is expressed on some subsets of naïve tissue resident
74 macrophages, including lung alveolar macrophages. Its role in antiviral macrophage responses is
75 largely unexplored. Here, we studied whether the differential expression of MARCO might
76 contribute to the varying susceptibility of macrophage subtypes to adenovirus.
77 We demonstrate that MARCO significantly enhances adenovirus infection and innate responses
78 in macrophages. These results help to understand adenoviral pathogenesis and may open new
79 possibilities to influence the outcome of infection with adenoviruses or adenovirus vectors.

Introduction

Virus – macrophage interactions play crucial roles in the pathogenesis and control of viral infections. Since intracellular pathogen sensing is central in the elicitation of early antiviral responses, early interactions of viral pathogens with innate immune cells, including macrophages, contribute significantly to effective antiviral defence mechanisms (1, 2). Macrophages differ in their origin, development and function (3). Since viruses use a range of surface molecules as receptors and facilitators for cellular entry (4), cell surface heterogeneity in macrophage subsets is expected to influence pathogen entry and also the innate stimulatory activity of different virus types.

Adenoviruses (Ad) are important, non-enveloped, double stranded DNA-containing pathogens. Replication-defective recombinant Ad vectors are used as vectors for vaccination against infectious diseases, for cancer immunotherapy and for studies of virus-host cell interactions (5, 6). Human Ad species C members (e.g. Ad type 2 and 5) are important tools in such applications (7, 8). Adenovirus infection elicits potent innate immune responses *in vitro* and *in vivo* and mononuclear phagocytes are major contributors to these responses (9). Different populations of tissue macrophages and dendritic cells produce high levels of pro-inflammatory cytokines and type I interferons in response to Ad particles. These responses can critically influence the course of natural Ad infection or the outcome of Ad vector applications, for example by tuning the expression of cell surface receptors on epithelial cells (10).

Virus entry triggers signaling pathways which play key roles in Ad-elicited pro-inflammatory responses but the contribution of cellular factors that mediate Ad entry into resident tissue macrophages, such as surface receptors, are incompletely understood (11, 12). The Coxsackie-Adenovirus receptor (CAR) and integrins are main surface receptors for Ad entry in epithelial

cells. *In vitro* studies have shown that Ads attach to these cells by the interaction of the viral fiber knob with CAR leading to the exposure of the membrane lytic protein-VI (13). Viruses are subsequently internalized via receptor mediated endocytosis, escape to the cytosol and import viral DNA into the nucleus (12, 14–17). In liver cells *in vivo*, Ad particles can also be internalized *via* binding to cell membrane heparan sulfate proteoglycans through blood factors (18, 19).

While macrophages and other myeloid cells do not express CAR, interactions with other host factors have been shown to contribute to Ad entry in these cells. This includes opsonization by serum factors such as antibodies or complement, leading to viral entry into macrophages and neutrophils via ubiquitously expressed Fc and complement receptors (20, 21). Contributions to virus entry by serum lactoferrin and the coagulation factor X have also been reported (19, 22). Furthermore, the scavenger receptors (SR) SR-A and SREC-I, members of pattern recognition receptors with broad ligand specificity and expressed ubiquitously on macrophages, have been implicated to play a role in Ad uptake in macrophages (21–25).

Several sensors have been implicated in the innate activation of mononuclear phagocytes by Ads. Toll Like Receptors (TLR) 2, 4 and 9 have been shown to contribute to Ad induced cytokine production (26, 27). Efficient triggering of innate responses was shown to require endosomal escape and cytoplasmic detection of the virus (28). Recently, the cyclic GMP-AMP synthase (cGAS) has been identified as a major cytosolic innate sensor for Ads (29, 30).

Previously, we have demonstrated that the production of innate cytokines to respiratory pathogens, including Ads, is significantly stronger in murine AMs and in non-transformed, GM-CSF-dependent, self-renewing AM-like macrophages (designated Max-Planck-Institute (MPI) cells) than in bone marrow derived macrophages (BMMs) (31). Similar to AMs, MPI cells express high levels of the SR class A protein MARCO while the rather Ad insensitive BMMs do

not express this scavenger receptor. Functionally, MARCO has been shown to directly enhance antibacterial macrophage responses (32). Whether it plays a similar role in macrophage responses to viral infections has not yet been investigated.

In this study, we investigated the possibility that MARCO expression enhances the susceptibility of macrophages to Ad. Using several mouse macrophage types, we show that the presence of MARCO allows rapid adenovirus gene expression and strong virus-stimulated innate responses, while blocking or the lack of MARCO, results in a strong impairment of these processes. Thus, MARCO is involved in innate Ad recognition and the elevated Ad sensitivity of MARCO-expressing macrophages is due to the expression of this receptor on the cell surface.

Results

Ad entry and the activation of innate signaling in MPI cells and AMs, unlike that in BMMs, is fast and efficient

Intracellular sensing of incoming virus particles is a major process in triggering antiviral responses. We tested the efficiency of adenoviral transduction of various macrophage types, i.e. alveolar macrophages (AMs), bone marrow-derived macrophages (BMMs) and MPI cells, using a non-replicating GFP-expressing adenovirus. The lung epithelial cell line A549 that can be infected efficiently with Ads was also used as a positive control. Microscopic examination of the cells 16 h post infection (p. i.) infection revealed that the majority of the MPI cells, AMs and A549 cells were strongly GFP positive, while BMMs expressed GFP only weakly (Fig. 1A). The time course of GFP expression in infected cells was analyzed by flow cytometry and showed that in A549, MPI cells and AMs GFP expression was detectable already 6h after infection, whereas at 10 h after infection, BMMs were still GFP negative (Fig. 1B). After 16 h, about 94 - 96 % of the A549, MPI cells and AMs expressed GFP. In MPI cells and AMs two populations, a moderately and a strongly positive subset could be identified. In contrast, only 75% of BMMs were weakly GFP-positive by this late time-point. These results demonstrated a faster and more efficient transduction of MPI cells and AMs compared to BMMs.

To compare the kinetics and strength of the Ad-induced signaling and cytokine responses in the different macrophage types, we measured the activation of the transcription factors IRF3 and NF-κB, the activation of the mitogen-activated protein kinase p38, and the secretion of IFN-α/β and IL-6 at various time points after Ad inoculation. Activation of p38 and IRF3 was analyzed using phospho-specific antibodies whereas nuclear translocation of the NF-κB subunit p65 was used to analyze NF-κB activation. In MPI cells, the strong activation of p38, IRF3 and NF-κB was first

detectable 1-2 h after infection, and persisted up to 8 h for NF-κB and at least up to 10 h for IRF3 and p38 (Fig. 2A). In contrast, in BMMs a weak, delayed and shorter activation of p38 was detected between 2 and 6 h and the activation of IRF3 and NF-κB was not detected at all (Fig. 2A). Consistent with this, Ad-infected MPI cells exhibited an early and strong production of type I interferon and IL-6, while only marginal production of these cytokines was observed 16 h after inoculation of BMMs (Fig. 2B). Murine AMs (Siglec F, F4/80 and CD11c triple positive cells), which constitute the vast majority of freshly isolated BAL cells (Fig. S1A), were also infected with Ad. Similar to the infection of MPI cells, and unlike that of BMMs, they exhibited early and strong phosphorylation of p38 and IRF3 (Fig. S1B) and a strong cytokine response (Fig. S1C). In summary, these results document a large difference in the activation of Ad-stimulated innate signaling between MPI cells/AMs and BMMs, and this correlates with the efficiency of Ad transduction.

Cytoplasmic sensing by the cyclic GMP-AMP synthase (cGAS) mediates Ad-stimulated innate responses in MPI cells

The initiation of Ad-induced innate responses has been attributed to the cell surface receptors TLR2 and 4, the endosomal TLR9, and more recently to the cytoplasmic DNA sensor cGAS (26, 27, 29). MPI cells deficient for both TLR2 and TLR4 showed no reduction of IL-6 production following Ad infection (Fig. 3A). Furthermore, infection of MPI cells with the Ad2 ts1 mutant virus, which is taken up into endosomes but does not enter the cytosol (33), did not induce detectable cytokine production (Fig. 3A), indicating that virus sensing at the plasma membrane or in the endosomes is not sufficient for the induction of the innate responses in MPI cells. To test the role of cytoplasmic cGAS, we used shRNA to knockdown this sensor in MPI cells. A C911 mismatch shRNA was used as a control (34). AdGFP transduction of cGAS knock-down cells

resulted in significantly decreased cytokine production compared to Ad-transduced MPI cells expressing a the C911 control shRNA (Fig. 3B). In a control experiment, cytokine production in response to LPS was not reduced in cGAS knock-down MPI cells (Fig. S2A). Notably, the knockdown of cGAS had no negative influence on the AdGFP transduction of MPI cells as measured by GFP expression in infected MPI cells (Fig. S2B).

Ad induced production of mature IL-1α in MPI cells, but not in BMMs

We have previously demonstrated that LPS-stimulated MPI macrophages, unlike BMMs, secrete substantial amounts of IL-1α (31). Ad infection also induced a significant IL-1α response, which peaked 8 h after inoculation, and a marginal IL-1β response in MPI cells, but not in BMMs (Fig. 4A). We tested whether Ad infection also induces the maturation of these cytokines. For this purpose, we infected MPI cells and BMMs with Ad, and analyzed the IL-1α and IL-1β forms in cell lysates at different times p. i. by Western blotting. Ad infection resulted in the processing of pre-existing immature IL-1α between 0.5 and 8 h p. i. and in the accumulation of pro-IL-1α, starting after 4 h of stimulation (Fig. 4B). Furthermore, immature IL-1β, but not the mature IL-1β form was induced in Ad-infected MPI cells at later time points (4-16 h. p.i.) (Fig. 4B). Finally, no induction of IL-1α or IL-1β was detectable in lysates of Ad-infected BMMs.

Blocking the scavenger receptor MARCO on MPI cells and AMs interferes with Ad entry and the induction of cytokine production.

We investigated whether the differential expression of a ligand recognition receptor might be responsible for the increased sensitivity of MPI cells and AMs to Ad compared to BMMs. As expected, the mRNA for CAR, the main receptor responsible for the uptake of species C Ads in

most non-immune cells, is not detectable in MPI cells and BMMs (Fig. S3A, B). Although the scavenger receptors SR-A and SREC1 have been implicated in Ad entry in macrophages (21–25), analysis of mRNA levels in MPI cells and BMMs did not show a strong expression of these genes in MPI cells (Fig. S3A, B), in agreement with our previously obtained microarray data (31). This suggested that these proteins are not involved in the differential sensitivity to Ad (Fig. S3). As shown in Fig. S3A-C and demonstrated previously (31, 35), another related microbial sensor, the scavenger receptor MARCO, is highly expressed in MPI cells, but absent in resting BMMs. SR-A is weakly expressed on both cell types (Fig. S3C). We also tested MARCO expression on various tissue resident macrophages. We found no significant MARCO expression in liver and skin macrophages. However, peritoneal macrophages, AMs and spleen marginal zone macrophages exhibited substantial levels of MARCO on their surface (Fig. S4). These cell types have previously been reported to be very efficiently infected by Ads (36–39). We tested a possible involvement of MARCO in the Ad transduction and in the elicitation of innate responses. For this purpose, we compared GFP expression and IL-1α and IL-6 responses of AdGFP-infected MPI cells and AMs in the presence or absence of a monoclonal antibody that blocks ligand binding to MARCO (40). Pre-incubation for 30 minutes with anti-MARCO, but not with a control antibody, almost completely abolished both the AdGFP transduction and the virus induced cytokine responses of these cell types (Fig. 5A, B). These results suggested a crucial role for MARCO in the Ad sensing in MPI cells and AMs.

Several serum proteins have been shown to mediate Ad uptake to myeloid cells previously (20, 22), however, scavenger receptors mediate ligand internalization without their help (32). So far, the Ad transduction of macrophages in this study was carried out in the presence of fetal calf serum. As shown in Fig. 5C, the absence of fetal calf serum did not reduce the GFP expression

(upper panel) or the IL-6 response (lower panel) of the infected cells. These results suggest that MARCO-expressing macrophages do not need opsonizing proteins to sense Ads.

MARCO deficiency drastically reduces the Ad transduction rate and the reactivity of MPI cells and AMs to the virus

To test the importance of MARCO for Ad transduction, we generated an MPI macrophage line from MARCO$^{-/-}$ mice. As expected, these cells expressed macrophage markers and responded to LPS (TLR4 ligand) and FSL-1 (TLR2 ligand) similarly as wt MPI cells (Fig. S5A, B). Importantly however; compared to wt MPI macrophages, MARCO$^{-/-}$ cells showed a strong reduction of Ad transduction (Fig. 6A, C) and Ad stimulated cytokine responses (Fig. 6B), while the Ad infection of MARCO deficient BMMs was not significantly reduced (Fig 6C). A similar Ad-insensitive phenotype was also exhibited by two other MARCO$^{-/-}$ MPI cell lines, generated independently (not shown). In addition, we isolated AMs from wt, MARCO$^{-/-}$, SR-A$^{-/-}$ and MARCO$^{-/-}$/ SR-A$^{-/-}$ double deficient mice and infected them with AdGFP. Compared to wt cells, MARCO$^{-/-}$ and MARCO$^{-/-}$/SR-A$^{-/-}$ AMs showed strongly reduced GFP expression (Fig. 6D) and lacked an IL-6 response (Fig. 6E). However, the loss of SR-A alone resulted in no reduction of GFP expression and only a moderate decrease of the IL-6 response in infected AMs (Fig. 6E). As expected, the expression of macrophage surface markers and the LPS responses of wt and MARCO$^{-/-}$ AMs were very similar (Fig. S5C, D). We also tested if MARCO expression contributes to Ad infection in peritoneal macrophages. We found that wt cells can be efficiently infected and activated (IL-6 response) by AdGFP; however, MARCO deficiency resulted in the marked reduction of AdGFP transduction and of virus triggered IL-6 response (Fig. 7). These results indicate that the absence of MARCO, but not SR-A, severely reduces Ad transduction and the innate responses in these macrophage types.

Transfection of MARCO in macrophages leads to increased Ad sensitivity

To provide further evidence for the importance of MARCO, we transfected the murine RAW 264.7 macrophage line that does not express MARCO (Fig. S6A, right) with a plasmid expressing the full length murine MARCO, or with the same expression vector lacking MARCO. In both cases, expression of the co-transfected reporter tomato gene allowed the discrimination between transfected (tomato positive) and non-transfected (tomato negative) cells. As shown in Fig. 8A, both transfections yielded approximately 33% tomato positive cells at the time of analysis. Transfection of RAW 264.7 cells with the MARCO-expressing plasmid resulted in MARCO surface expression only in tomato-positive cells (Fig. S6A, left). MARCO was absent in both tomato-positive and -negative cells transfected with the control plasmid, (Fig. S6A, left). MARCO- and control-transfected cells were infected with AdGFP and analyzed 8 hours post inoculation for GFP and tomato expression by flow cytometry. While 50 % of the MARCO-transfected, tomato-positive cells expressed GFP, less than 10 % of control-transfected, tomato-positive cells expressed GFP, indicating a dramatic increase of Ad transduction due to the expression of MARCO. Pearson´s data analysis revealed a moderate positive correlation ($r=0.34$; $P<0.0001$) of GFP and tomato expression in MARCO transfected RAW264.7 cells, whereas no significant correlation ($r=-0.02$; $P=0.3361$) was found for the control transfected cells (Fig. S6B). Furthermore, only cultures containing the MARCO-transfected cells produced high levels of IL-6 in response to AdGFP (Fig. 8B).

Discussion

In the present study, we show that when compared to BMMs, Ad infects mouse alveolar macrophages and the alveolar macrophage-like MPI cells significantly more strongly and with an accelerated kinetics. This higher infectivity rate explains why the Ad-induced pro-inflammatory cytokine responses in the two latter macrophage types are substantially higher than in BMMs. Previous studies indicated the possible involvement of cell surface TLR2, 4, endosomal TLR9 and non-TLR cytosolic virus sensing in the Ad stimulated innate cytokine responses (26–28). Using gene-deficient cells and the endosomal penetration-defective mutant virus Ad2 ts1, we excluded a significant involvement of TLR2, 4 and of endosomal sensing in the Ad-triggered responses of MPI cells. Earlier, we showed that the IFN-α/β and IL-6 responses elicited by Ad strictly require viral endosomal escape (28). Here, we show that Ad transduction is much more efficient in MPI cells and AMs than in BMMs. This implies that both the delivery of viral particles to the cytosol and the nuclear import of viral DNA are efficient in these cells. Since incoming viral DNA is frequently and to a high level mis-delivered to the cytosol (17), these results explain why the triggering of innate signalling, such as the activation of NF-κB, IRF-3 and p38, and the induction of cytokine responses are faster and stronger in AMs and MPI cells than in BMMs. The use of a different, less efficient Ad internalisation route in BMM may be responsible for the lack of detectability of NF-κB and IRF-3 activation upon infection and therefore for a very weak cytokine response. This is consistent with our previous results, and results of others, showing that significantly higher Ad doses are necessary to elicit potent cytokine responses in BMMs (28, 41).

The finding that Ad ts1, a virus mutant unable to enter the cytosol does not induce an IL-6 response in MPI cells confirms that Ad-triggered responses need cytosolic virus sensing. We show here that the knockdown of the cytosolic DNA sensor cGAS impairs the ability of Ads to activate MPI cells, but does not affect adenoviral transduction measured by GFP transgene expression. These findings are in agreement with the major role of cytoplasmic virus sensing in MPI cells and with recent data showing that cGAS is a dominant Ad sensor for the induction of IFN-αβ, but not for the nuclear translocation of the viral DNA in murine MS1 and RAW 264.7 cell lines (29).

A likely explanation for the considerable differences in the kinetics of transduction between AMs and MPI cells and those in BMMs was the differential expression of a specific cell surface receptor. The scavenger receptor MARCO, which is highly expressed in alveolar, peritoneal and MPI macrophages but not in BMMs (31) appeared to be a suitable candidate. Indeed, our data demonstrate that the loss of function of MARCO, achieved either by MARCO-blocking antibodies or by MARCO knockout in AMs and MPI macrophages, both lead to severely reduced expression of Ad-transduced GFP and Ad-induced cytokine production. Moreover, the introduction of MARCO into RAW 264.7 macrophages, which do not express this protein, rendered the cells susceptible to Ad transduction and contributed to increased cytokine production. Thus, MARCO is decisively involved in the susceptibility of macrophages to Ad.

In the past, MARCO was shown to mediate the direct binding and internalization of various non-opsonized particles. Antibodies to the ligand-binding domain of this receptor can block the interaction (35). In agreement, our data obtained with MPI cells reveal that Ad infection and the elicitation of innate responses by Ad does not require the presence of serum but can be inhibited by the MARCO blocking antibody. Therefore, it is likely that MARCO, similar to its role in the

uptake of other microbial and non-microbial agents, mediates the internalization of adenovirus and thus promotes subsequent innate responses. This may occur in cooperation with other plasma membrane proteins. A cooperative action of the Ad receptor CAR with integrins has been shown previously to initiate viral entry in epithelial cells (13). Tissue resident macrophages are very heterogeneous (3) and variable expression of the factors responsible for Ad uptake and transduction, including MARCO, may explain the observed wide range of Ad infectibility of the polyclonal MPI cells, AMs and peritoneal macrophages.

SR-A, a scavenger receptor related to MARCO and commonly expressed in various macrophage types, has been reported to be involved in the uptake of Ad by macrophages (21–25). Here, the comparison of GFP expression and cytokine production in AdGFP-infected alveolar macrophages from wt, $MARCO^{-/-}$, $SR\text{-}A^{-/-}$ and $MARCO^{-/-}/SR\text{-}A^{-/-}$ mice indicated that this receptor, either alone or in combination with MARCO, does not play a major role in the Ad infection or activation of this macrophage type.

The identification of MARCO involvement in the susceptibility of cells to Ad agrees well with previous studies demonstrating that AMs and splenic marginal zone macrophages, which strongly express MARCO, trap Ad particles very early after infection (36, 39).

Ad induced *in vivo* IL-1α production has been demonstrated previously in spleen. Di Paolo et al. showed that MARCO-positive spleen marginal zone macrophages are a source of IL-1α in Ad infected mice (36). They have also shown Ad stimulated, IL-1α-mediated biological responses and the nuclear translocation of IL-1α. However, proteolytic maturation of this cytokine has not been demonstrated because similar to the N-terminal pro-piece ppIL-1α, the immature IL-1α precursor can also readily translocate into the nucleus (42). As shown previously (31) and in the present study, MARCO-expressing AMs and MPI cells also exhibit a robust IL-1α response upon

infection with Ads. We provide direct evidence for the intracellular processing of IL-1α in Ad-infected MPI cells. Both the full length and the processed IL-1α forms are biologically active, although the pro-inflammatory activity of the mature IL-1α protein is higher (43). Since Ads are important respiratory pathogens (44), and IL-1α has been shown to play a central role in lung pathologies induced by several microbial agents (45, 46), the elucidation of the mechanisms of Ad-induced IL-1α production in lung alveolar macrophages is likely to have medical significance. Previously, di Paolo et al. (37) demonstrated that Il-1α produced by MARCO-expressing splenic marginal zone macrophages is responsible for splenic neutrophil recruitment and the subsequent elimination of virus-infected cells. Thus, similar mechanisms may contribute to the AM-mediated control of respiratory Ad infection.

While MARCO is known to be involved in the innate sensing of various bacteria, much less is known about its role in virus infection and antiviral defence. Recently, MARCO was shown to play a role in the entry of HSV and vaccinia viruses into keratinocytes but macrophage infection and antiviral innate responses were not investigated (47, 48). MARCO was also shown to indirectly suppress early antiviral responses by removing cellular debris in the course of influenza infection (49). In contrast, our studies demonstrate a positive role for MARCO in the direct mediation of virus infection and triggering of antiviral responses in macrophages. Thus, MARCO may influence antiviral innate responses in a virus type specific manner.

The expression of MARCO in specific subsets of naïve tissue resident macrophages can be important for the primary sensing of naturally occurring viral infections. AMs represent an early line of defense against respiratory pathogens; thus, the mechanisms shown here may critically influence the early stages of natural adenovirus infection. In addition, MARCO expression can be induced by inflammatory stimuli in macrophages normally not expressing this receptor (50). This

may broaden the macrophage types contributing to the clearance of viral pathogens during the later phases of infection.

Our findings imply potential beneficial and harmful effects in medical applications using recombinant adenoviruses. MARCO-mediated Ad infection of mononuclear phagocytes could contribute directly to efficient antigen processing and presentation. The cytokine responses induced by the vector could also provide adjuvant effects for vaccination. However, MARCO mediated innate responses may be damaging, if the inflammatory response is too strong. Furthermore, certain MARCO sensed pathogens, such as Ad and mycobacteria, induce hypersensitivity to LPS and to other TLR ligands (51–53). Exposure of hypersensitive individuals to TLR-triggering pathogens may lead to uncontrolled inflammatory reactions and in the worst case to septic shock and death (54).

Our findings present a new target for further analyses of Ad-macrophage interactions. Future studies delineating the details of the Ad-MARCO interaction may provide tools to beneficially influence both naturally occurring Ad infections as well as therapeutic approaches utilizing this viral vector.

Materials & Methods

Mouse Strains. C57BL/6 (wt) and C57BL/6 MARCO$^{-/-}$, C57BL/6 SR-A$^{-/-}$ and C57BL/6 MARCO$^{-/-}$/SR-A$^{-/-}$ mice (50) were bred under specific pathogen-free conditions at the Max-Planck Institute Freiburg or at the University Hospital Rheinisch-Westfälische Technische Hochschule Aachen. Knock-out mice strains were originally provided to S.G. by K. Tryggvason, Karolinska Institute, Stockholm, Sweden. Procedures were in accordance with institutional, state and federal guidelines on animal welfare.

Cell culture, Adenovirus infection and MARCO blocking. Murine AMs were isolated by bronchoalveolar lavage, and BMMs and fetal liver-derived MPI cells were generated as described (31). Murine peritoneal cells were obtained by lavage with 5 ml PBS. Murine spleen cell suspensions were obtained by mechanical disintegration. To obtain skin cells, mouse ears were digested with Liberase TM (Roche) as described in (55). Minced mouse livers were digested with Liberase TM (Roche) for 30 min at 37°C and Kupffer cells were further enriched by gradient centrifugation, as described in (56). The A549 adenocarcinoma derived human alveolar basal epithelial cells and RAW 264.7 murine macrophages were cultured in DMEM (Gibco) supplemented with 10% FCS (Biochrom), 100 µg/ml streptomycin (Gibco), 100 U/ml penicillin (Gibco) and 10 mM HEPES (Gibco). For the induction of cytokines, all cell types were used at a density of 5 x 10^5 cells/ml and plated on 96-well microtiter plates (Nunc) or 6-well plates (Nunc). For adenovirus infection, the replication-deficient green fluorescent protein-expressing species C human Ad5 virus (AdGFP), the species C human wt Ad2 or the mutant Ad2 ts1 were used. All viruses were used at a concentration of 1000 particles/cell if not stated otherwise. GFP transduction was assessed using fluorescence and phase contrast microscopy or FACS. The viruses were propagated and purified with $CsCl_2$ density gradient ultracentrifugation as described

405 (57). The concentration of virus particles was determined using a spectrophotometer. OD
406 260−OD 330=1 corresponds to 10^{12} virus particles/ml and the ratio of viral particles to plaque
407 forming units was 20:1.
408 LPS from *S. minnesota* R595 (Enzo life sciences) was used at a concentration of 100 ng/ml.
409 MARCO ligand binding was blocked by incubation of cells with purified anti-mouse MARCO
410 antibody (clone ED31, AbD Serotec) at a concentration of 20 ng/µl for 30 minutes prior to
411 AdGFP infection. A purified rat anti-mouse IL-4 (clone 11B11, BD Biosciences) was used as an
412 isotype control.
413 **shRNA-mediated knockdown of cGAS in retrovirus transduced MPI cells.** The following
414 plasmids were generously provided by Eric Campeau (pENTRpTER$^+$ Addgene plasmid #17453,
415 pCQXIN X2 DEST Addgene plasmid #17399) and a published protocol was followed (58). Viral
416 RNAi for mcGAS, and its C911 control, were established as described (34). The following
417 oligos were designed using the Invitrogen shRNA block-it tool (Life Technologies) and
418 purchased from Microsynth Switzerland: mcGAS (adapted from (59)):
419 mshcGAS_for 5'GATCCCGGATTGAGCTACAAGAATAGTGTGCTGTCCTATTCTTGT
420 AGCTCAATCCTTTTTGGAAA-3', mshcGAS_rev 5'AGCTTTTCCAAAAAGGATTGAG
421 CTACAAGAATAGGACAGCACACTATTCTTGTAGCTCAATCCGG-3', mshcGAS_
422 C911_for 5'-GATCCCGGATTGAGGATCAAGAATAGTGTGCTGTCCTATTCTTGATC
423 CTCAATCCTTTTTGGAAA-3', mshcGAS_C911_rev 5'AGCTTTTCCAAAAAGGATTGA
424 GGATCAAGAATAGGACAGCACACTATTCTTGATCCTCAATCCGG-3'.
425 shRNAs were cloned into the entry vector pENTRpTER$^+$ and recombined into the MMLV-
426 destination vector pCQXIN X2 DEST using Gateway cloning with LR clonase. Plasmids were
427 validated by sequencing. VSV-G-pseudotyped MLV retroviruses were generated according to

standard procedure in HEK 293T cells and used to produce stably transduced MPI cells using G418 selection. Knockdown efficiency was 80%.

FACS analysis. Nonspecific binding was blocked by pre-incubation of the cells with anti-CD16/CD32 antibody (93, BioLegend) in 1% goat serum in PBS. MARCO was detected with purified mouse MARCO antibody (ED31, AbD Serotec) in combination with Alexa Fluor 647-conjugated goat anti-rat IgG (Molecular Probes). Fluorophore-conjugated CD11b (M1/70) and CD14 (Sa14-2), CD11c (N418), F4/80 (BM8), CD45 (30-F11), antibodies were from BioLegend, Siglec F (E50-2440) from BD Biosciences, SignR1 (ERTR9) and SR-A (2F8) from AbD Serotec. Data were acquired on a BD FACSCanto II cytometer and analyzed with FlowJo software (Tree Star).

Western blotting. Cell lysates were prepared in the presence of phosphatase inhibitor mixture II (Sigma), protease inhibitor cocktail (Sigma) and PMSF (Sigma) using 100 µl of the respective lysis buffer per 10^6 cells. RIPA buffer (20 mM TRIS pH 7.5, 150 mM NaCl, 1 % NP40, 0,5 % DOC, 1 mM EDTA, 0,1 % SDS) was used to prepare whole cell lysates or the cells were fractionated for cytosolic and nuclear fractions as described (31). The quality of fractionation was checked using anti-GAPDH (6C5, Acris Antibodies) and polyclonal rabbit anti-histone 3 antibodies (Merck Millipore) as described previously (31). Protein samples were blotted to nitrocellulose membranes after denaturing SDS-polyacrylamide gel electrophoresis. The following antibodies were used for immunoblotting: rabbit anti-NFkB p65 (C-20, Santa Cruz Biotechnology), rabbit anti-phospho-IRF3 (Ser396)(4D4G, Cell Signaling Technology), rabbit anti-phospho-p38 MAPK (Thr180/Tyr182) (12F8, Cell Signaling Technology), polyclonal goat anti-IL-1α (R&D Systems), hamster anti-IL-1α (ALF-161, Santa Cruz Biotechnology), hamster anti-IL-1β (B122, RD Systems) horseradish peroxidase-conjugated goat anti-mouse and goat anti-rabbit IgG (both Cell Signaling Technology), mouse anti-hamster IgG (Santa Cruz

Biotechnology) and rabbit anti-goat IgG (Jackson Immunoresearch). Blots were developed with the SuperSignal West Pico Chemiluminescent Substrate (Thermo Scientific).

Cytokine detection. IL-6, IL-1α and IL-1β were quantified in cell free culture supernatants by ELISA using antibody pairs from BD Pharmingen (IL-6, IL-1β) and Ebioscience (IL-1alpha) according to the instructions of the manufacturer. IFN-α/β was measured with reference to a recombinant mouse IFN-β standard using an established luciferase expression based bioassay as described (28).

Transfection. The mammalian expression vector pCmarcoiT was used to express the full length murine MARCO protein. To construct the vector, full length MARCO cDNA was amplified from MPI cell cDNA using the forward primer 5'-gccatgggaagtaaacaactcc-3' and the reverse primer 5'-gtcaggagcattccacacccgca-3' and cloned to give a CMV-driven bicistronic transcript with the tandem-dimer Tomato gene (henceforth referred to as tomato) expressed from an internal translation initiation site. This allows FACS identification and analysis of the transfected cells. RAW 264.7 cells were transfected using TurboFect Transfection Reagent (Thermo Scientific) according to manufacturer's instructions.

Quantitative RT-PCR. RNA was prepared using Tri reagent (Sigma) according to the manufacturer's instructions. SuperScript II Reverse Transcriptase (Invitrogen) was used to reverse-transcribe 2 µg of RNA. Real-time RT–PCR was performed using LightCycler® 480 SYBR Green I Master kit (Roche) and the Roche LightCycler 480 instrument with the following primers: Marco: fw: 5'-ACCAGGCCTACCAGGTTTG- 3', rev: 5'-ACCCTGCACTCCAGGTTTT- 3'; Sra: fw: 5'-CAGTCAGCATCCTCTTGTTCA- 3', rev: 5'-GTCTTCTTTACCAGCAATGACAAA- 3'; Srec1: fw: 5'-GACTGGACCCGAAGGACA- 3', rev: 5'-CGAGCCCAAGTTGGTGAG- 3'; CAR: fw: 5'- CCCTGGGGTTGCAAATAAG- 3', rev: 5'- GATCCATCCACGAAGCATCT- 3'; Actin: fw: 5'-

476 GTCCACACCCGCCACCAGTTCG- 3,' rev: 5'-GGAATACAGCCCGGGGAGCATCGTC- 3'.
477 Data was normalized to β-actin expression and plotted on a relative scale for each gene by setting
478 the cells with the highest level of expression to 100 %.
479 **Data analysis, Pearson correlation and statistics.** Data were analyzed with Graphpad Prism 5.0
480 software. Data are represented as mean and error bars show the standard error of the mean.
481 Statistical significance was calculated using the unpaired t-test (*: P <0.05; **: P < 0.01; ***: P<
482 0.001). If not stated otherwise, the figures show representative results of at least 3 independent
483 experiments.

Acknowledgments

We thank J. Ippisch, P. Lüderitz and M. Mitterer, M. Kauffmann and A. Fodor for technical assistance and T. Wilhelm for technical instructions. We thank P. Stäheli and A. Babler for organizational help. We are deeply thankful to C. Galanos for discussions and continuous support. C.G. passed away on July 9th 2015.

Funding information

G.F. received financial support from the NC3Rs (NC/L00058X/1) and W.W.S. from the Deutsche Forschungsgemeinschaft (DFG) through EXC294 (the Centre for Biological Signalling Studies, BIOSS). I.C. was supported by an Alexander von Humboldt fellowship. UFG, MS, NS were supported by the Swiss National Science Foundation (310030B_160316), and the European Commission Initial Training Network (FP7; ADVance no. 290002).The funders had no role in study design, data collection and interpretation, or the decision to submit the work for publication.

500 **References**

501

502 1. Goubau D, Deddouche S, Reis e Sousa C. 2013. Cytosolic Sensing of Viruses. Immunity
503 38:855–869.

504 2. Mercer J, Greber UF. 2013. Virus interactions with endocytic pathways in macrophages
505 and dendritic cells. Trends Microbiol 21:380–388.

506 3. Gordon S, Plüddemann A, Martinez Estrada F. 2014. Macrophage heterogeneity in
507 tissues: phenotypic diversity and functions. Immunol Rev 262:36–55.

508 4. Yamauchi Y, Greber UF. 2016. Principles of Virus Uncoating: Cues and the Snooker
509 Ball. Traffic n/a-n/a.

510 5. Bell J, McFadden G. 2014. Viruses for tumor therapy. Cell Host Microbe 15:260–265.

511 6. Rollier CS, Reyes-Sandoval A, Cottingham MG, Ewer K, Hill AVS. 2011. Viral vectors
512 as vaccine platforms: deployment in sight. Curr Opin Immunol 23:377–382.

513 7. Appaiahgari MB, Vrati S. 2015. Adenoviruses as gene/vaccine delivery vectors: promises
514 and pitfalls. Expert Opin Biol Ther 15:337–351.

515 8. Wold WSM, Toth K. 2013. Adenovirus vectors for gene therapy, vaccination and cancer
516 gene therapy. Curr Gene Ther 13:421–433.

517 9. Hendrickx R, Stichling N, Koelen J, Kuryk L, Lipiec A, Greber UF. 2014. Innate
518 Immunity to Adenovirus. Hum Gene Ther 25:265–284.

519 10. Lütschg V, Boucke K, Hemmi S, Greber UF. 2011. Chemotactic antiviral cytokines
520 promote infectious apical entry of human adenovirus into polarized epithelial cells. Nat
521 Commun 2:391.

522 11. Fejer G, Freudenberg M, Greber UF, Gyory I. 2011. Adenovirus-triggered innate
523 signalling pathways. Eur J Microbiol Immunol 1:279–288.

12. Wolfrum N, Greber UF. 2013. Adenovirus signalling in entry. Cell Microbiol 15:53–62.

13. Burckhardt CJ, Suomalainen M, Schoenenberger P, Boucke K, Hemmi S, Greber UF. 2011. Drifting motions of the adenovirus receptor CAR and immobile integrins initiate virus uncoating and membrane lytic protein exposure. Cell Host Microbe 10:105–117.

14. Wiethoff CM, Nemerow GR. 2015. Adenovirus membrane penetration: Tickling the tail of a sleeping dragon. Virology 479–480:591–599.

15. Suomalainen M, Greber UF. 2013. Uncoating of non-enveloped viruses. Curr Opin Virol 3:27–33.

16. Luisoni S, Suomalainen M, Boucke K, Tanner LB, Wenk MR, Guan XL, Grzybek M, Coskun Ü, Greber UF. 2015. Co-option of Membrane Wounding Enables Virus Penetration into Cells. Cell Host Microbe 18:75–85.

17. Flatt JW, Greber UF. 2015. Misdelivery at the Nuclear Pore Complex-Stopping a Virus Dead in Its Tracks. Cells 4:277–296.

18. Parker AL, Waddington SN, Nicol CG, Shayakhmetov DM, Buckley SM, Denby L, Kemball-Cook G, Ni S, Lieber A, McVey JH, Nicklin SA, Baker AH. 2006. Multiple vitamin K-dependent coagulation zymogens promote adenovirus-mediated gene delivery to hepatocytes. Blood 108:2554–2561.

19. Shayakhmetov DM, Gaggar A, Ni S, Li Z-Y, Lieber A. 2005. Adenovirus Binding to Blood Factors Results in Liver Cell Infection and Hepatotoxicity. J Virol 79:7478–7491.

20. Cotter MJ, Zaiss AK, Muruve DA. 2005. Neutrophils Interact with Adenovirus Vectors via Fc Receptors and Complement Receptor 1. J Virol 79:14622–14631.

21. Xu Z, Tian J, Smith JS, Byrnes AP. 2008. Clearance of Adenovirus by Kupffer Cells Is Mediated by Scavenger Receptors, Natural Antibodies, and Complement. J Virol 82:11705–11713.

548 22. Adams WC, Bond E, Havenga MJE, Holterman L, Goudsmit J, Karlsson Hedestam GB,
549 Koup RA, Loré K. 2009. Adenovirus serotype 5 infects human dendritic cells via a
550 coxsackievirus–adenovirus receptor-independent receptor pathway mediated by
551 lactoferrin and DC-SIGN. J Gen Virol 90:1600–1610.
552 23. Haisma HJ, Boesjes M, Beerens AM, van der Strate BWA, Curiel DT, Plüddemann A,
553 Gordon S, Bellu AR. 2009. Scavenger Receptor A: A New Route for Adenovirus 5. Mol
554 Pharm 6:366–374.
555 24. Piccolo P, Vetrini F, Mithbaokar P, Grove NC, Bertin T, Palmer D, Ng P, Brunetti-Pierri
556 N. 2013. SR-A and SREC-I Are Kupffer and Endothelial Cell Receptors for Helper-
557 dependent Adenoviral Vectors. Mol Ther 21:767–774.
558 25. Khare R, Reddy VS, Nemerow GR, Barry MA. 2012. Identification of Adenovirus
559 Serotype 5 Hexon Regions That Interact with Scavenger Receptors. J Virol 86:2293–
560 2301.
561 26. Doronin K, Flatt JW, Paolo NCD, Khare R, Kalyuzhniy O, Acchione M, Sumida JP, Ohto
562 U, Shimizu T, Akashi-Takamura S, Miyake K, MacDonald JW, Bammler TK, Beyer RP,
563 Farin FM, Stewart PL, Shayakhmetov DM. 2012. Coagulation Factor X Activates Innate
564 Immunity to Human Species C Adenovirus. Science 338:795–798.
565 27. Appledorn DM, Patial S, McBride A, Godbehere S, Rooijen NV, Parameswaran N,
566 Amalfitano A. 2008. Adenovirus Vector-Induced Innate Inflammatory Mediators, MAPK
567 Signaling, As Well As Adaptive Immune Responses Are Dependent upon Both TLR2 and
568 TLR9 In Vivo. J Immunol 181:2134–2144.
569 28. Fejer G, Drechsel L, Liese J, Schleicher U, Ruzsics Z, Imelli N, Greber UF, Keck S,
570 Hildenbrand B, Krug A, Bogdan C, Freudenberg MA. 2008. Key Role of Splenic Myeloid
571 DCs in the IFN-?? Response to Adenoviruses In Vivo. PLoS Pathog 4.

572 29. Lam E, Stein S, Falck-Pedersen E. 2014. Adenovirus Detection by the
573 cGAS/STING/TBK1 DNA Sensing Cascade. J Virol 88:974–981.
574 30. Lau L, Gray EE, Brunette RL, Stetson DB. 2015. DNA tumor virus oncogenes antagonize
575 the cGAS-STING DNA-sensing pathway. Science 350:568–571.
576 31. Fejer G, Wegner MD, Gyory I, Cohen I, Engelhard P, Voronov E, Manke T, Ruzsics Z,
577 Dolken L, Prazeres da Costa O, Branzk N, Huber M, Prasse A, Schneider R, Apte RN,
578 Galanos C, Freudenberg MA. 2013. Nontransformed, GM-CSF-dependent macrophage
579 lines are a unique model to study tissue macrophage functions. Proc Natl Acad Sci U S A
580 110:E2191–E2198.
581 32. Areschoug T, Gordon S. 2009. Scavenger receptors: role in innate immunity and
582 microbial pathogenesis. Cell Microbiol 11:1160–1169.
583 33. Imelli N, Ruzsics Z, Puntener D, Gastaldelli M, Greber UF. 2009. Genetic reconstitution
584 of the human adenovirus type 2 temperature-sensitive 1 mutant defective in endosomal
585 escape. Virol J 6:174.
586 34. Buehler E, Chen Y-C, Martin S. 2012. C911: A bench-level control for sequence specific
587 siRNA off-target effects. PloS One 7:e51942.
588 35. Palecanda A, Paulauskis J, Al-Mutairi E, Imrich A, Qin G, Suzuki H, Kodama T,
589 Tryggvason K, Koziel H, Kobzik L. 1999. Role of the Scavenger Receptor MARCO in
590 Alveolar Macrophage Binding of Unopsonized Environmental Particles. J Exp Med
591 189:1497–1506.
592 36. Di Paolo NC, Miao EA, Iwakura Y, Kaja M-K, Aderem A, Flavell RA, Papayannopoulou
593 T, Shayakhmetov DM. 2009. Virus sensing at the Plasma Membrane Triggers Interleukin-
594 1α–Mediated Pro-inflammatory Macrophage Response in vivo. Immunity 31:110–121.

595 37. Di Paolo NC, Baldwin LK, Irons EE, Papayannopoulou T, Tomlinson S, Shayakhmetov
596 DM. 2014. IL-1α and complement cooperate in triggering local neutrophilic inflammation
597 in response to adenovirus and eliminating virus-containing cells. PLoS Pathog
598 10:e1004035.
599 38. Yamaguchi T, Kawabata K, Koizumi N, Sakurai F, Nakashima K, Sakurai H, Sasaki T,
600 Okada N, Yamanishi K, Mizuguchi H. 2007. Role of MyD88 and TLR9 in the Innate
601 Immune Response Elicited by Serotype 5 Adenoviral Vectors. Hum Gene Ther 18:753–
602 762.
603 39. Zsengeller Z, Otake K, Hossain S-A, Berclaz P-Y, Trapnell BC. 2000. Internalization of
604 Adenovirus by Alveolar Macrophages Initiates Early Proinflammatory Signaling during
605 Acute Respiratory Tract Infection. J Virol 74:9655–9667.
606 40. Laan LJW van der, Döpp EA, Haworth R, Pikkarainen T, Kangas M, Elomaa O, Dijkstra
607 CD, Gordon S, Tryggvason K, Kraal G. 1999. Regulation and Functional Involvement of
608 Macrophage Scavenger Receptor MARCO in Clearance of Bacteria In Vivo. J Immunol
609 162:939–947.
610 41. Nociari M, Ocheretina O, Schoggins JW, Falck-Pedersen E. 2007. Sensing Infection by
611 Adenovirus: Toll-Like Receptor-Independent Viral DNA Recognition Signals Activation
612 of the Interferon Regulatory Factor 3 Master Regulator. J Virol 81:4145–4157.
613 42. Cohen I, Rider P, Carmi Y, Braiman A, Dotan S, White MR, Voronov E, Martin MU,
614 Dinarello CA, Apte RN. 2010. Differential release of chromatin-bound IL-1alpha
615 discriminates between necrotic and apoptotic cell death by the ability to induce sterile
616 inflammation. Proc Natl Acad Sci U S A 107:2574–2579.

617 43. Afonina IS, Tynan GA, Logue SE, Cullen SP, Bots M, Lüthi AU, Reeves EP, McElvaney
618 NG, Medema JP, Lavelle EC, Martin SJ. 2011. Granzyme B-dependent proteolysis acts as
619 a switch to enhance the proinflammatory activity of IL-1α. Mol Cell 44:265–278.
620 44. Marcos MA, Esperatti M, Torres A. 2009. Viral pneumonia. Curr Opin Infect Dis 22:143–
621 147.
622 45. Mayer-Barber KD, Andrade BB, Oland SD, Amaral EP, Barber DL, Gonzales J, Derrick
623 SC, Shi R, Kumar NP, Wei W, Yuan X, Zhang G, Cai Y, Babu S, Catalfamo M, Salazar
624 AM, Via LE, Barry Iii CE, Sher A. 2014. Host-directed therapy of tuberculosis based on
625 interleukin-1 and type I interferon crosstalk. Nature 511:99–103.
626 46. Caffrey AK, Lehmann MM, Zickovich JM, Espinosa V, Shepardson KM, Watschke CP,
627 Hilmer KM, Thammahong A, Barker BM, Rivera A, Cramer RA, Obar JJ. 2015. IL-1α
628 Signaling Is Critical for Leukocyte Recruitment after Pulmonary Aspergillus fumigatus
629 Challenge. PLoS Pathog 11.
630 47. MacLeod DT, Nakatsuji T, Wang Z, di Nardo A, Gallo RL. 2014. Vaccinia Virus Binds
631 to the Scavenger Receptor MARCO on the Surface of Keratinocytes. J Invest Dermatol.
632 48. MacLeod DT, Nakatsuji T, Yamasaki K, Kobzik L, Gallo RL. 2013. HSV-1 exploits the
633 innate immune scavenger receptor MARCO to enhance epithelial adsorption and
634 infection. Nat Commun 4:1963.
635 49. Ghosh S, Gregory D, Smith A, Kobzik L. 2011. MARCO Regulates Early Inflammatory
636 Responses against Influenza. Am J Respir Cell Mol Biol 45:1036–1044.
637 50. Chen Y, Wermeling F, Sundqvist J, Jonsson A-B, Tryggvason K, Pikkarainen T, Karlsson
638 MCI. 2010. A regulatory role for macrophage class A scavenger receptors in TLR4-
639 mediated LPS responses. Eur J Immunol 40:1451–1460.

640 51. Bowdish DME, Sakamoto K, Kim M-J, Kroos M, Mukhopadhyay S, Leifer CA,
641 Tryggvason K, Gordon S, Russell DG. 2009. MARCO, TLR2, and CD14 Are Required
642 for Macrophage Cytokine Responses to Mycobacterial Trehalose Dimycolate and
643 Mycobacterium tuberculosis. PLoS Pathog 5.
644 52. Fejér G, Szalay K, Gyory I, Fejes M, Kúsz E, Nedieanu S, Páli T, Schmidt T, Siklódi B,
645 Lázár G, Lázár G, Duda E. 2005. Adenovirus infection dramatically augments
646 lipopolysaccharide-induced TNF production and sensitizes to lethal shock. J Immunol
647 Baltim Md 1950 175:1498–1506.
648 53. Freudenberg MA, Kalis C, Chvatchko Y, Merlin T, Gumenscheimer M, Galanos C. 2003.
649 Role of interferons in LPS hypersensitivity. J Endotoxin Res 9:308–312.
650 54. Freudenberg MA, Tchaptchet S, Keck S, Fejer G, Huber M, Schütze N, Beutler B,
651 Galanos C. 2008. Lipopolysaccharide sensing an important factor in the innate immune
652 response to Gram-negative bacterial infections: Benefits and hazards of LPS
653 hypersensitivity. Immunobiology 213:193–203.
654 55. Weber FC, Németh T, Csepregi JZ, Dudeck A, Roers A, Ozsvári B, Oswald E, Puskás
655 LG, Jakob T, Mócsai A, Martin SF. 2015. Neutrophils are required for both the
656 sensitization and elicitation phase of contact hypersensitivity. J Exp Med 212:15–22.
657 56. Li P, Li J, Li M, Gong J, He K. 2014. An efficient method to isolate and culture mouse
658 Kupffer cells. Immunol Lett 158:52–56.
659 57. Fejer G, Gyory I, Tufariello J, Horwitz MS. 1994. Characterization of transgenic mice
660 containing adenovirus early region 3 genomic DNA. J Virol 68:5871–5881.
661 58. Campeau E, Ruhl VE, Rodier F, Smith CL, Rahmberg BL, Fuss JO, Campisi J, Yaswen
662 P, Cooper PK, Kaufman PD. 2009. A Versatile Viral System for Expression and
663 Depletion of Proteins in Mammalian Cells. PLoS ONE 4.

59. Wu J, Sun L, Chen X, Du F, Shi H, Chen C, Chen ZJ. 2013. Cyclic GMP-AMP is an endogenous second messenger in innate immune signaling by cytosolic DNA. Science 339:826–830.

60. Keck S, Müller I, Fejer G, Savic I, Tchaptchet S, Nielsen PJ, Galanos C, Huber M, Freudenberg MA. 2011. Absence of TRIF Signaling in Lipopolysaccharide-Stimulated Murine Mast Cells. J Immunol 186:5478–5488.

671 **Figure legends**

672

673 FIG 1. Efficiency of Ad infection in different cell types. (A) GFP expression was analyzed in
674 different cell types 16 h after infection with AdGFP using fluorescence (top) and light (phase
675 contrast; bottom) microscopy. Bars indicate 50 μm. (B) FACS analysis of GFP expression in
676 infected cells at the indicated time points. The number indicates the frequency of GFP+ cells 16 h
677 after infection, the gate indicates GFP+ cells.
678 FIG 2. Early immune activation of MPI cells and BMMs after infection with AdGFP. (A)
679 Western blot analysis of the cytoplasmic (p-p38, p-IRF3) or nuclear (NF-kB p65) cell fractions at
680 the indicated time points. (B) Cytokine production was measured by ELISA in cell free
681 supernatants at the indicated time points.
682 FIG 3. Ad-induced cytokine production in MPI cells is independent of TLR2/4 but dependent on
683 cGAS. (A) IL-6 induction in wt and TLR2/4$^{-/-}$ MPI cells after infection with wt Ad2 or mutant
684 Ad2 ts1. (B) Cytokine induction in cGAS-knockdown MPI cells inoculated with AdGFP or mock
685 for 16 h.
686 FIG 4. Ad-induced IL-1 production in MPI cells and BMMs. (A) Induction of IL-1α and IL-1β
687 in cell free supernatants of MPI cells and BMMs after Ad infection at the indicated time points.
688 (B) Western blot analysis of MPI and BMM cell lysates at the indicated time points.
689 FIG 5. Ad transduction is strongly reduced by blocking MARCO but independent of serum
690 factors. (A) GFP expression of cells infected with AdGFP in the presence of a MARCO-blocking
691 (right) or isotype antibody (left). Scale bars indicate 100 μm. Top: fluorescence, bottom: phase
692 contrast. (B) Cytokine production of AdGFP infected cells without antibody (control), MARCO-
693 blocking antibody or isotype control. (C) GPF expression (upper panel, fluorescence and

694 corresponding phase contrast) and IL-6 production (lower panel) of AdGFP infected MPI cells in
695 the presence or absence of fetal calf serum (FCS). Scale bars indicate 100 µm.
696 FIG 6. Effect of MARCO and SR-A deficiency on the expression of GFP and IL-6 production in
697 macrophages infected for 18 h with AdGFP. (A) Fluorescence microscopy (top) and
698 corresponding phase contrast (bottom) of infected $MARCO^{-/-}$ and wt MPI cells. Scale bars
699 indicate 50 µm. (B) IL-6 concentration in supernatants of mock-infected and infected $MARCO^{-/-}$
700 and wt MPI cells. (C) FACS comparison of $MARCO^{-/-}$ (grey filled histogram) and wt (open
701 histogram) MPI cells and BMM 16 h after infection with AdGFP. (D) Fluorescence microscopy
702 (top) and corresponding phase contrast (bottom) of mock-infected and infected AMs from
703 different knock-out mice. Scale bars indicate 100 µm. (E) IL-6 concentration in supernatants
704 from mock-infected and infected AMs obtained from different knockout mice.
705 Fig 7. Peritoneal cells from naive wt and $MARCO^{-/-}$ mice were infected with AdGFP *in vitro*.
706 Left: histograms of peritoneal macrophages 16 h after infection (black: $MARCO^{-/-}$, red: wt,
707 dotted: mock , lines: Ad, right: IL-6 induction.
708 FIG 8. Expression of MARCO in RAW264.7 macrophages increases the infection efficiency and
709 cytokine response to Ad. (A) Cells infected with AdGFP 16 h after transfection with murine
710 MARCO or control plasmid DNA. Tomato was used as a reporter for successfully transfected
711 cells. Cells were analyzed 8 h post infection by FACS. (B) IL-6 was analyzed in cell free
712 supernatants 8 h after AdGFP infection.
713
714 **Supplementary figure legends**
715
716 FIG S1. AdGFP-induced innate immune activation of freshly isolated murine AMs. (A) AM
717 gating strategy. Living immune cells were identified as DAPI negative, CD45 (pan-immune cell

718 marker) expressing BAL cells. AMs were further identified as Siglec F / F4/80 double positive
719 cells and comprised the large majority of immune cells (> 95 %). AMs highly expressed CD11c
720 but no CD11b. (B) Activation of p38 and IRF3 was analyzed in whole-cell-lysates by western
721 blot analysis at the indicated time points. (C) IFN-α/β and IL-6 were analyzed by ELISA in cell
722 free supernatants 16 h post infection.
723 FIG S2. LPS-induced IL-6 production and Ad-induced GFP expression are independent of cGAS.
724 (A) MPI cells were transduced with cGAS or control shRNA and stimulated with 100 ng/ml LPS.
725 IL-6 was analyzed in cell free supernatants 16 h after stimulation. (B) GFP expression in MPI
726 cells infected with AdGFP for 16 h after shRNA mediated knockdown of cGAS (top:
727 fluorescence; bottom: corresponding phase contrast, Scale bars indicate 100 μm).
728 FIG S3. CAR, SREC1, SR-A and MARCO expression in BMM and MPI cells. (A) Comparison
729 of mRNA expression (normalized intensity values; NI) in BMM and MPI cells using microarray
730 data published in (1).
731 (B) mRNA expression of indicated genes validated by qRT-PCR. Lung and B cell total RNA was
732 used as positive and negative control, respectively. n. d.: not detectable (C) FACS analysis of SR-
733 A and MARCO expression in BMM and MPI cells . Open histograms: specific antibody, grey
734 filled histograms: isotype control.
735 FIG S4. MARCO expression of different tissue macrophages. Macrophages were analyzed
736 immediately after digestion (liver, skin, spleen) or lavage (peritoneum, lung) without prior
737 enrichment by selective adhesion.
738 FIG S5. Surface protein expression and innate responsiveness of wt and $MARCO^{-/-}$ MPI cells and
739 AM. (A) FACS analysis with anti-CD11b, -CD14, -MARCO, -Siglec F, -F4/80 and -CD11c.
740 Open black histograms: wt cells, open red histograms: $MARCO^{-/-}$ cells, grey filled histograms:
741 isotype control (B) IL-6 production in cell free supernatants of MPI cells 16 h after stimulation

742 with FSL-1 or LPS. (C) FACS analysis of BAL cells from naive wt and MARCO$^{-/-}$ mice. AMs
743 were identified as Siglec F / F4/80 double positive cells as shown in Fig S1A and AM number is
744 given as frequency of CD45 (pan-immune cell marker) positive BAL cells. AMs were FACS
745 analyzed with anti-CD11b, -CD14, -Siglec F, -F4/80 and -CD11c. Open, black histograms: wt
746 cells, open red histograms: MARCO$^{-/-}$ cells, grey filled histograms: isotype control (D) IL-6
747 production in cell free supernatants of AMs 16 h after stimulation with 100 ng/ml LPS.
748 FIG S6. Analysis of transfected RAW264.7 cells. (A) FACS analysis of RAW264.7 cells
749 transfected with MARCO/tomato- or tomato-expressing plasmids. FACS analysis with anti-
750 MARCO was performed 16 h after transfection. Left: Frequencies of tomato+ cells. Right:
751 MARCO staining on tomato+ (top) or tomato- (bottom) cell populations (open histogram:
752 tomato-transfected cells, grey filled histogram: MARCO/tomato -transfected cells). (B) Scatter
753 dot plot of linear regression of AdGFP infected MARCO or control transfected RAW264.7 cells.
754

755 **Supplementary references**

756

757 **1.** Fejer G, Wegner MD, Györy I, Cohen I, Engelhard P, Voronov E, Manke T, Ruzsics Z,
758 Dölken L, da Costa OP. 2013. Nontransformed, GM-CSF–dependent macrophage lines
759 are a unique model to study tissue macrophage functions. Proceedings of the National
760 Academy of Sciences **110:**E2191-E2198.

761

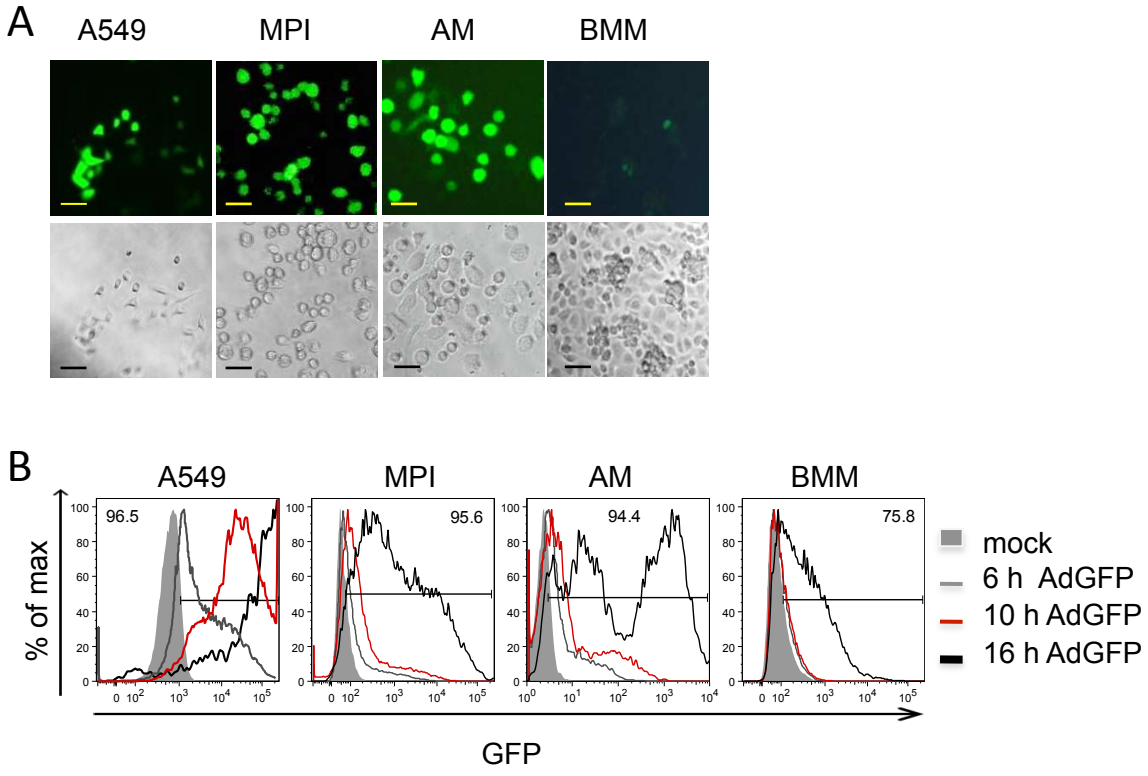

FIG 1. Efficiency of Ad infection in different cell types. (A) GFP expression was analyzed in different cell types 16 h after infection with AdGFP using fluorescence (top) and light (phase contrast; bottom) microscopy. Bars indicate 50 µm. (B) FACS analysis of GFP expression in infected cells at the indicated time points. The number indicates the frequency of GFP+ cells 16 h after infection, the gate indicates GFP+ cells.

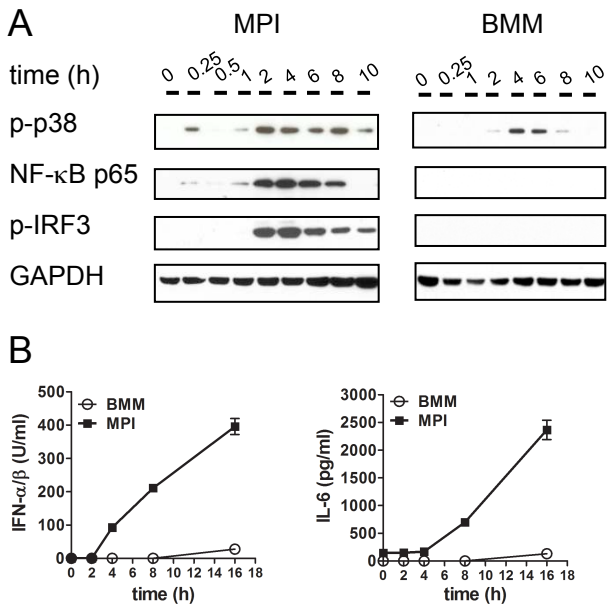

FIG 2. Early immune activation of MPI cells and BMMs after infection with AdGFP. (A) Western blot analysis of the cytoplasmic (p-p38, p-IRF3) or nuclear (NF-kB p65) cell fractions at the indicated time points. (B) Cytokine production was measured by ELISA in cell free supernatants at the indicated time points.

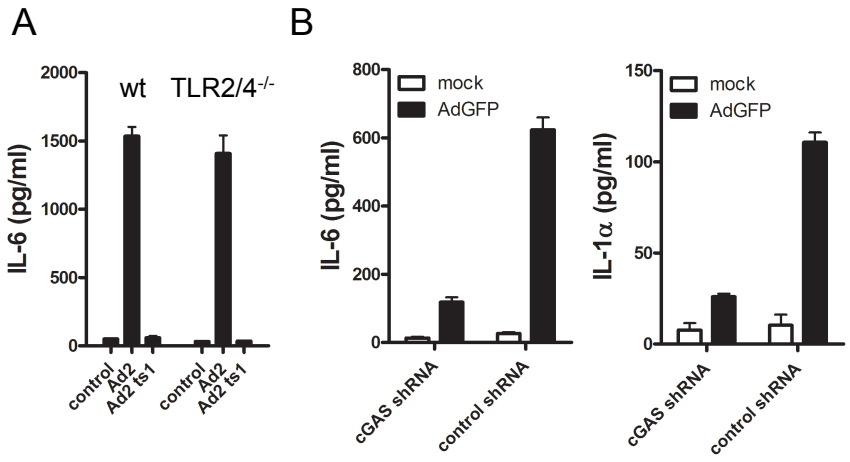

FIG 3. Ad-induced cytokine production in MPI cells is independent of TLR2/4 but dependent on cGAS. (A) IL-6 induction in wt and TLR2/4$^{-/-}$ MPI cells after infection with wt Ad2 or mutant Ad2 ts1. (B) Cytokine induction in cGAS-knockdown MPI cells inoculated with AdGFP or mock for 16 h.

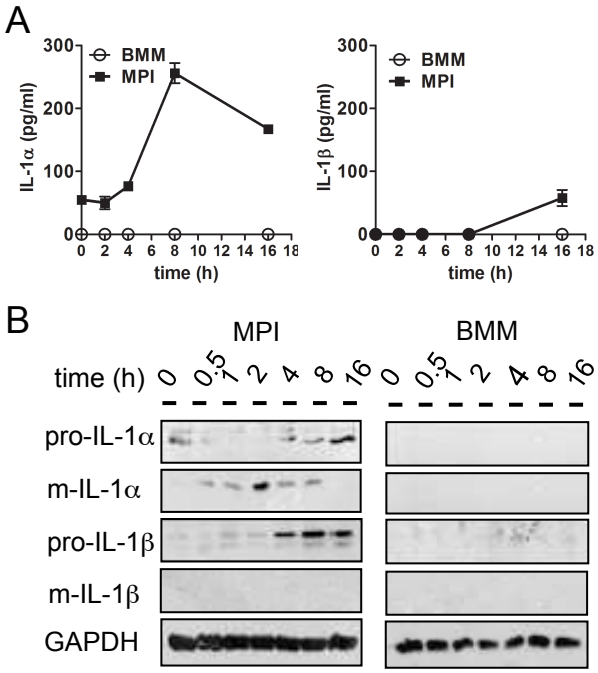

FIG 4. Ad-induced IL-1 production in MPI cells and BMMs. (A) Induction of IL-1α and IL-1β in cell free supernatants of MPI cells and BMMs after Ad infection at the indicated time points. (B) Western blot analysis of MPI and BMM cell lysates at the indicated time points.

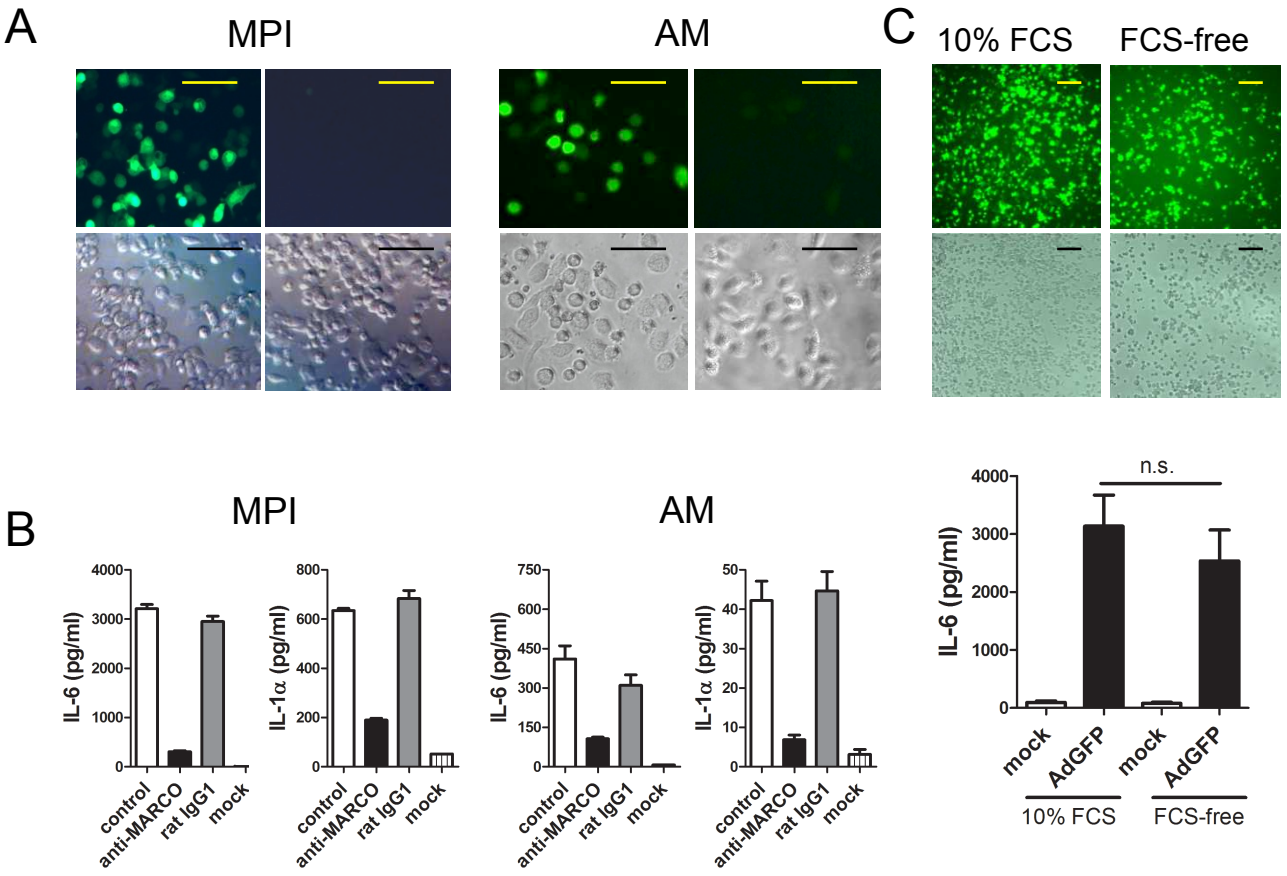

FIG 5. Ad transduction is strongly reduced by blocking MARCO but independent of serum factors. (A) GFP expression of cells infected with AdGFP in the presence of a MARCO-blocking (right) or isotype antibody (left). Scale bars indicate 100 µm. Top: fluorescence, bottom: phase contrast. (B) Cytokine production of AdGFP infected cells without antibody (control), MARCO-blocking antibody or isotype control. (C) GPF expression (upper panel, fluorescence and corresponding phase contrast) and IL-6 production (lower panel) of AdGFP infected MPI cells in the presence or absence of fetal calf serum (FCS). Scale bars indicate 100 µm.

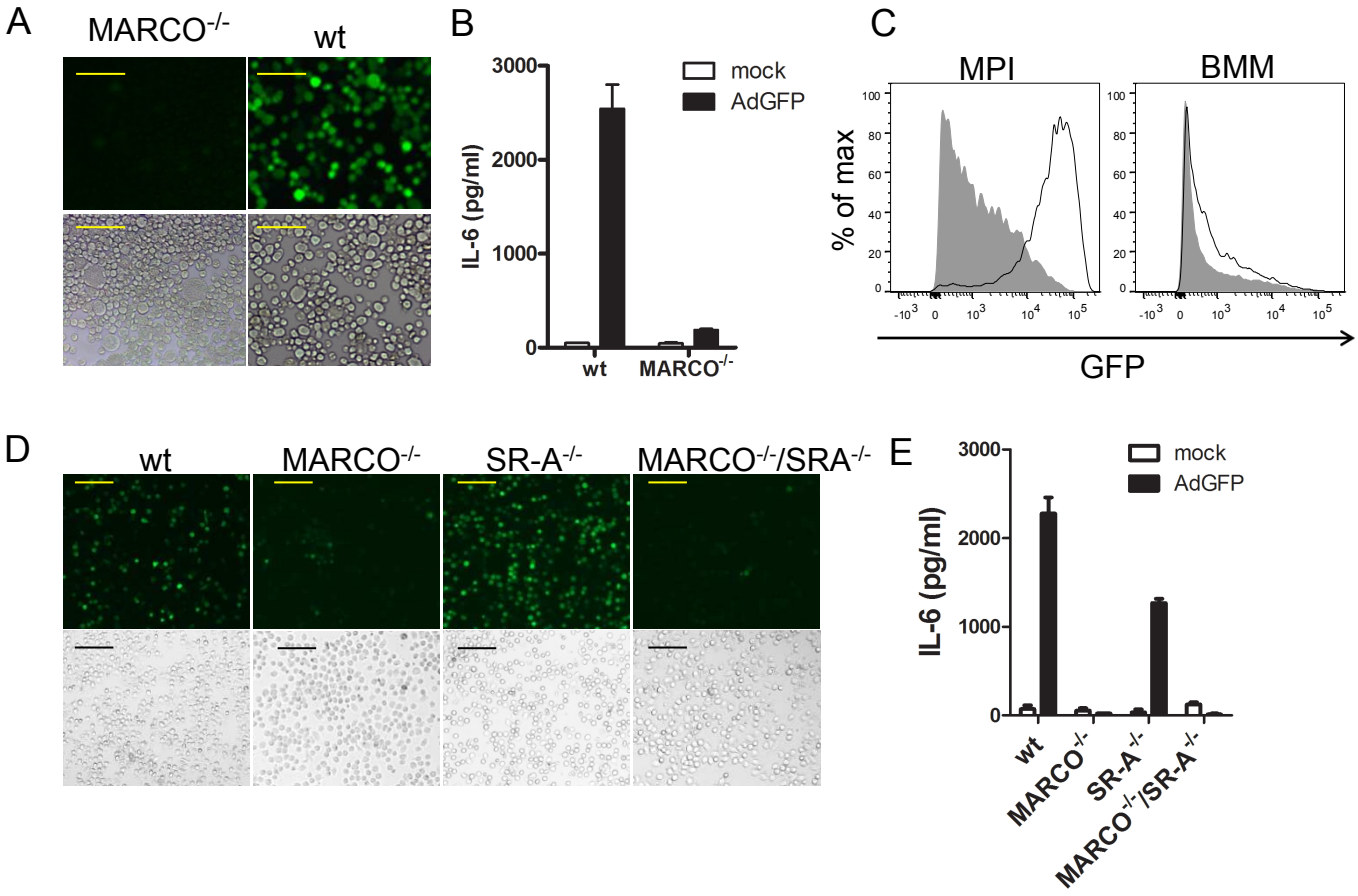

FIG 6. Effect of MARCO and SR-A deficiency on the expression of GFP and IL-6 production in macrophages infected for 18 h with AdGFP. (A) Fluorescence microscopy (top) and corresponding phase contrast (bottom) of infected MARCO$^{-/-}$ and wt MPI cells. Scale bars indicate 50 µm. (B) IL-6 concentration in supernatants of mock-infected and infected MARCO$^{-/-}$ and wt MPI cells. (C) FACS comparison of MARCO$^{-/-}$ (grey filled histogram) and wt (open histogram) MPI cells and BMM 16 h after infection with AdGFP. (D) Fluorescence microscopy (top) and corresponding phase contrast (bottom) of mock-infected and infected AMs from different knock-out mice. Scale bars indicate 100 µm. (E) IL-6 concentration in supernatants from mock-infected and infected AMs obtained from different knockout mice.

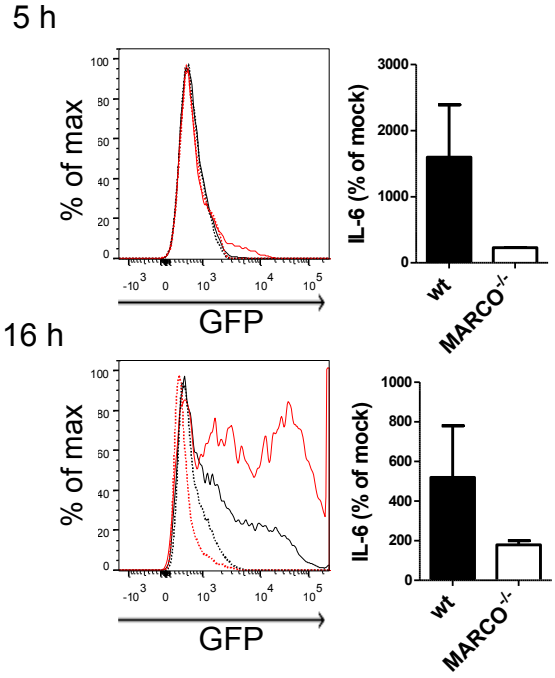

FIG 7. Peritoneal cells from naive wt and MARCO$^{-/-}$ mice were infected with AdGFP *in vitro*. Left: histograms of peritoneal macrophages 16 h after infection (black: MARCO$^{-/-}$, red: wt, dotted: mock , lines: Ad, right: IL-6 induction

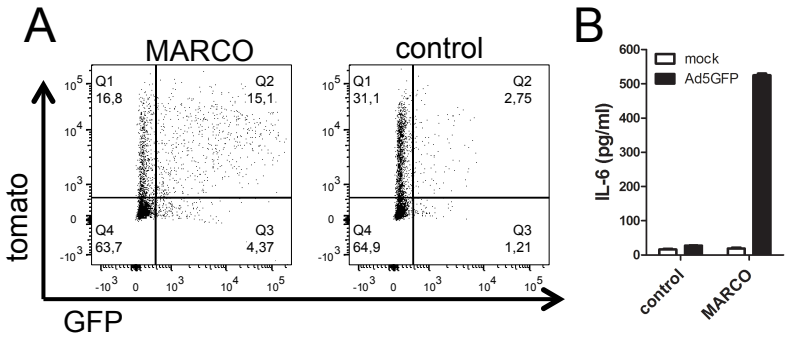

FIG 8. Expression of MARCO in RAW264.7 macrophages increases the infection efficiency and cytokine response to Ad. (A) Cells infected with AdGFP 16 h after transfection with murine MARCO or control plasmid DNA. Tomato was used as a reporter for successfully transfected cells. Cells were analyzed 8 h post infection by FACS. (B) IL-6 was analyzed in cell free supernatants 8 h after AdGFP infection.

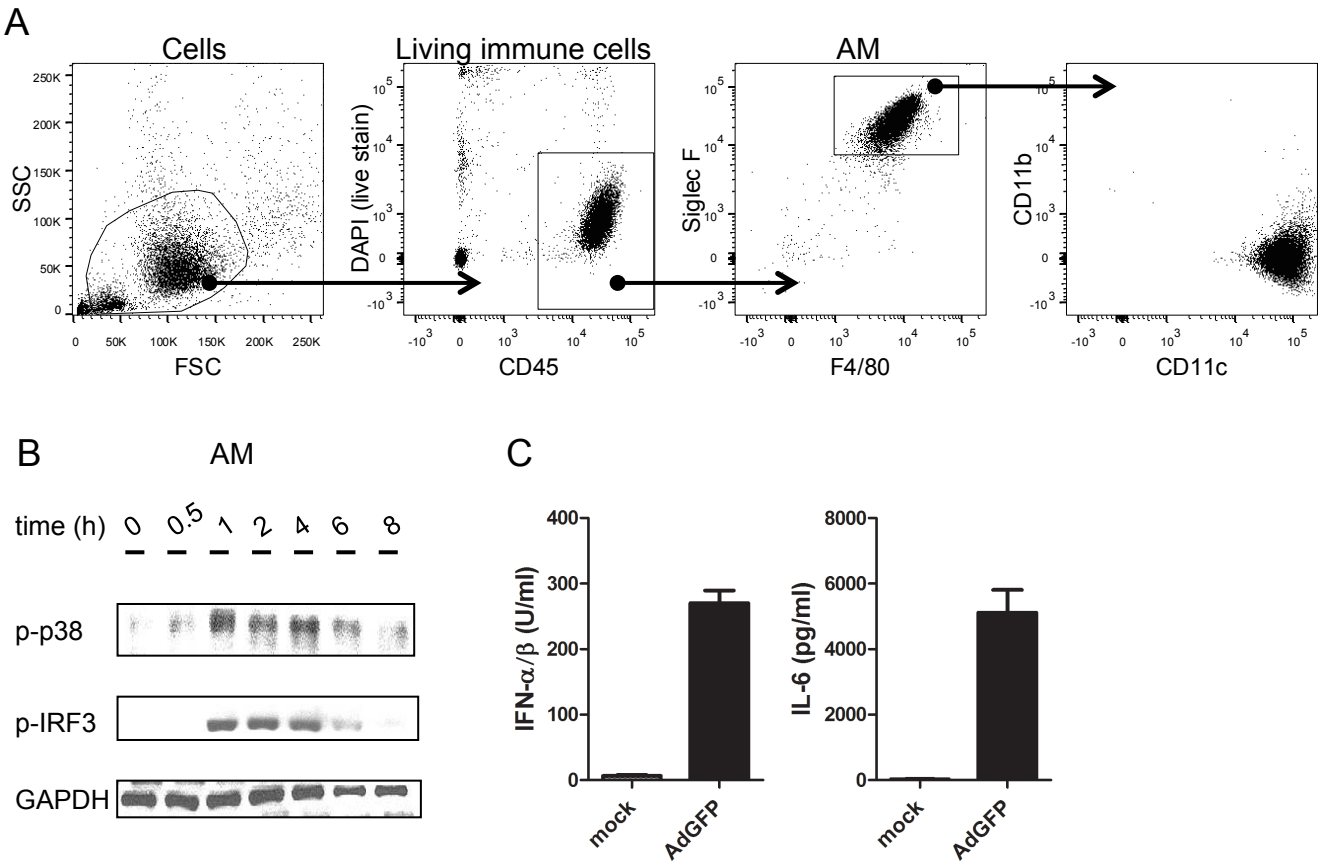

FIG S1. AdGFP-induced innate immune activation of freshly isolated murine AMs. (A) AM gating strategy. Living immune cells were identified as DAPI negative, CD45 (pan-immune cell marker) expressing BAL cells. AMs were further identified as Siglec F / F4/80 double positive cells and comprised the large majority of immune cells (> 95 %). AMs highly expressed CD11c but no CD11b. bottom: comparison of AM frequency before and after selective adhesion. (B) Activation of p38 and IRF3 was analyzed in whole-cell-lysates by western blot analysis at the indicated time points. (C) IFN-α/β and IL-6 were analyzed by ELISA in cell free supernatants 16 h post infection.

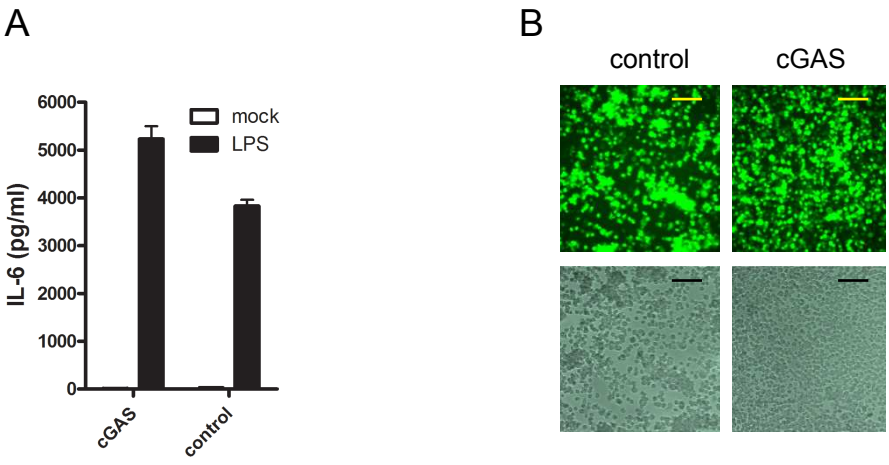

FIG S2. LPS-induced IL-6 production and Ad-induced GFP expression are independent of cGAS. (A) MPI cells were transduced with cGAS or control shRNA and stimulated with 100 ng/ml LPS. IL-6 was analyzed in cell free supernatants 16 h after stimulation. (B) GFP expression in MPI cells infected with AdGFP for 16 h after shRNA mediated knockdown of cGAS (top: fluorescence; bottom: corresponding phase contrast, Scale bars indicate 100 μm).

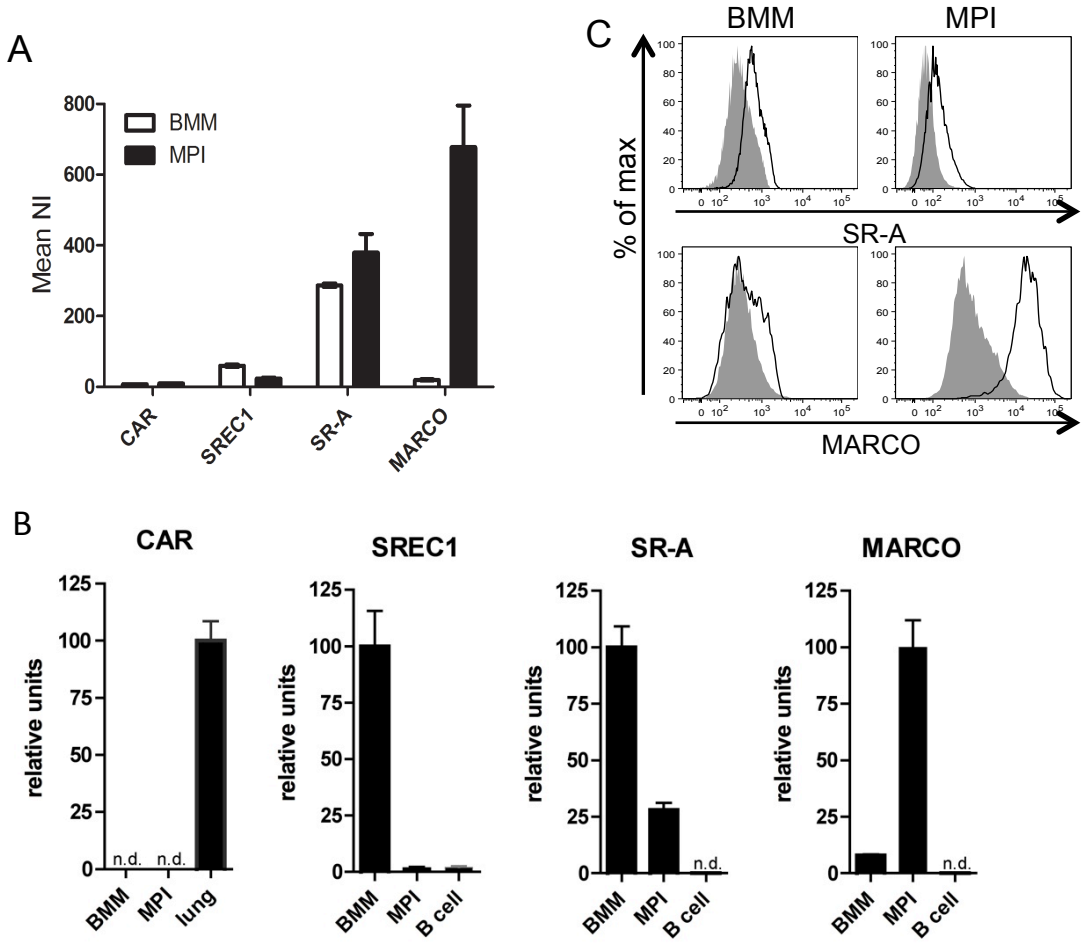

FIG S3. CAR, SREC1, SR-A and MARCO expression in BMM and MPI cells. (A) Comparison of mRNA expression (normalized intensity values; NI) in BMM and MPI cells using microarray data published in (1).

(B) mRNA expression of indicated genes validated by qRT-PCR. Lung and B cell total RNA was used as positive and negative control, respectively. n. d.: not detectable (C) FACS analysis of SR-A and MARCO expression in BMM and MPI cells . Open histograms: specific antibody, grey filled histograms: isotype control

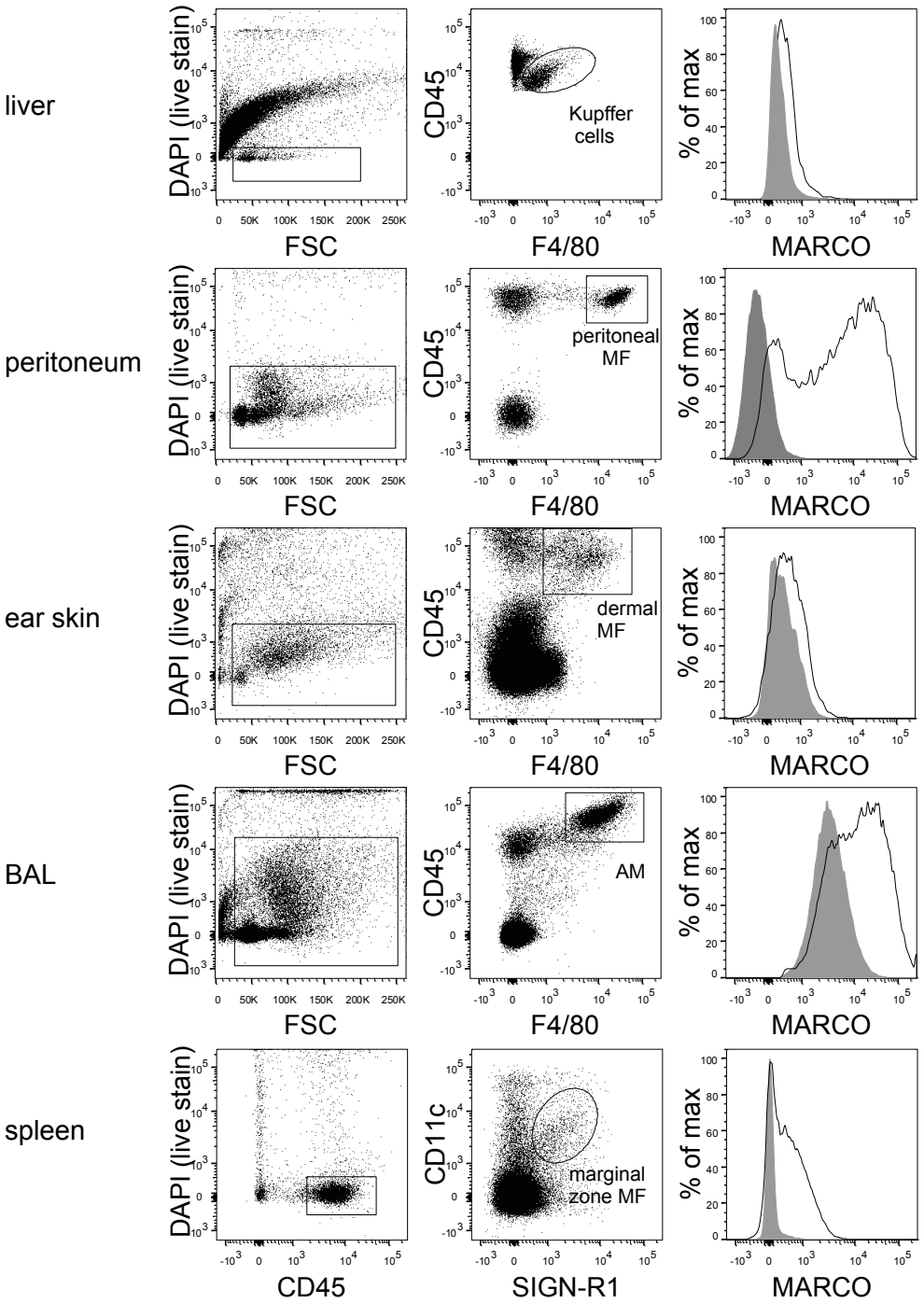

FIG S4. MARCO expression of different tissue macrophages. Macrophages were analyzed immediately after digestion (liver, skin, spleen) or lavage (peritoneum, lung) without prior enrichment by selective adhesion.

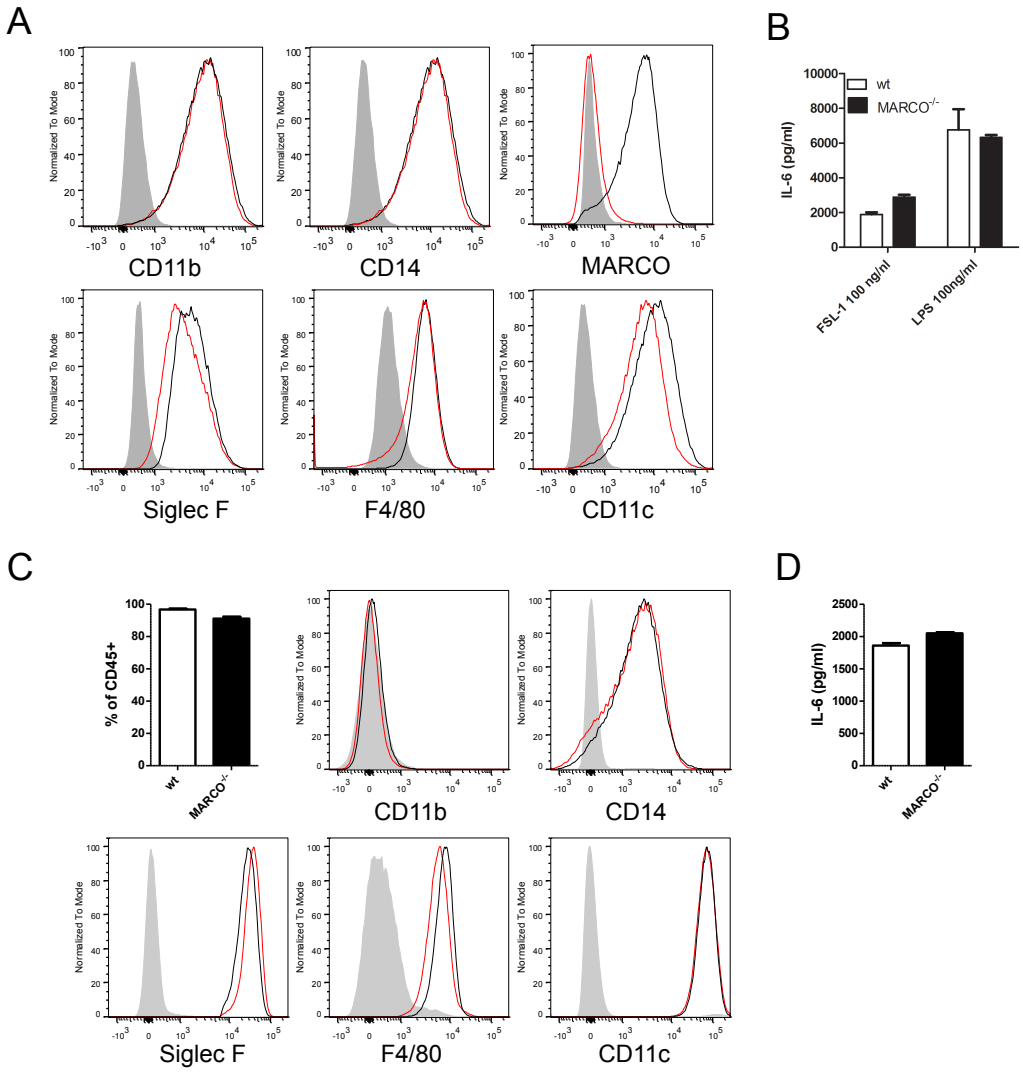

FIG S5. Surface protein expression and innate responsiveness of wt and MARCO$^{-/-}$ MPI cells and AM. (A) FACS analysis with anti-CD11b, -CD14, -MARCO, -Siglec F, -F4/80 and -CD11c. Open black histograms: wt cells, open red histograms: MARCO-/- cells, grey filled histograms: isotype control (B) IL-6 production in cell free supernatants of MPI cells 16 h after stimulation with FSL-1 or LPS. (C) FACS analysis of BAL cells from naïve wt and MARCO$^{-/-}$ mice. AMs were identified as Siglec F / F4/80 double positive cells as shown in Fig S1A and AM number is given as frequency of CD45 (pan-immune cell marker) positive BAL cells. AMs were FACS analyzed with anti-CD11b, -CD14, -Siglec F, -F4/80 and -CD11c. Open, black histograms: wt cells, open red histograms: MARCO$^{-/-}$ cells, grey filled histograms: isotype control (D) IL-6 production in cell free supernatants of AMs 16 h after stimulation with 100 ng/ml LPS.

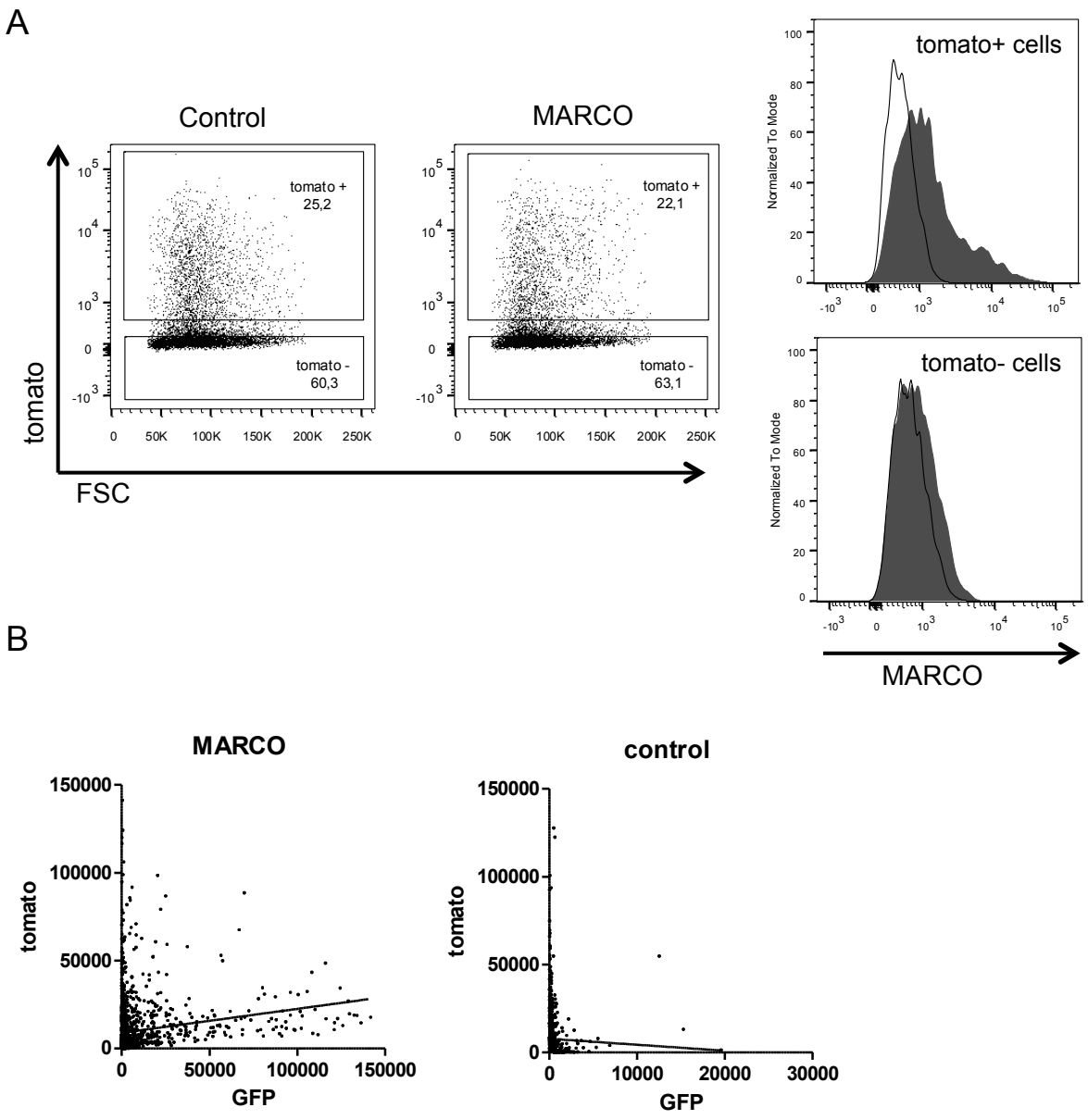

FIG S6. Analysis of transfected RAW264.7 cells. (A) FACS analysis of RAW264.7 cells transfected with MARCO/tomato- or tomato-expressing plasmids. FACS analysis with anti-MARCO was performed 16 h after transfection. Left: Frequencies of tomato+ cells. Right: MARCO staining on tomato+ (top) or tomato- (bottom) cell populations (open histogram: tomato-transfected cells, grey filled histogram: MARCO/tomato -transfected cells). (B) Scatter dot plot of linear regression of AdGFP infected MARCO or control transfected RAW264.7 cells.